UNIVERSITY OF CALIFORNIA SAN DIEGO

Effects of Osmotic Pressures and TRPV-4 Inhibitors on Calcium Levels in Dorsal Root Ganglion Cells

A thesis submitted in partial satisfaction of the requirements for the degree Master of Science

in

Bioengineering

by

Albert D. Chen

Committee in Charge:
Professor Sameer Shah, Chair
Professor Kevin King, Co-Chair
Professor Ester Kwon

2019

The Thesis of Albert D. Chen is approved, and it is acceptable in quality and form for publication on microfilm and electronically:

_____

_____

Co-Chair

_____

Chair

University of California San Diego

2019

Table of Contents

List of Figures

List of Tables

Acknowledgements

I would like to acknowledge Dr. Sameer Shah for his support and for serving as the chair of my committee. He allowed me to pursue a thesis in a field of my interest and take ideas from his grant to do research on. His guidance through this project was significant and taught me many ways of analytical thinking.

I would also like to acknowledge Dr. Kevin King and Dr. Ester Kwon for participating on my committee.

I would also like to thank Elisabeth Orozco and Stephanie Adachi for providing lab tips and teaching me protocols needed for this project. I could not have asked for better collaborators.

ABSTRACT OF THE THESIS

Effects of Osmotic Pressures and TRPV-4 Inhibitors on Calcium Levels in Dorsal Root Ganglion Cells

By

Albert D. Chen

Master of Science in Bioengineering

University of California San Diego, 2019

Professor Sameer Shah, Chair

Professor Kevin King, Co-Chair

Cancer is a prevalent disease that has been researched for many years to find a cure. A potential focus is the popular chemotherapeutic, paclitaxel (PTX), which has been known to treat a number of metastatic cancers with high efficacy. However, PTX induces neuropathy that results in acute pain, muscle weakness, among other symptoms. This has caused research to delve into the effects of PTX and the ability to halt these symptoms when using it for treatment. Several studies have shown that PTX influences the activity of TRPV-4, a mechanically gated calcium ion channel, and there has been evidence that suggests that intracellular calcium signals are involved in the pathogenesis of peripheral neuropathy caused by PTX. In coincidence, if TRPV-4 inhibition in dorsal root ganglion cells (DRGs) can be proved with fruition, this can potentially reduce cell death in DRGs. Because of PTX's potential effect on TRPV-4 channels, it is important to determine if inhibiting these channels would have any effect on calcium dynamics. Pretreatment of wild-type mice DRGs with TRPV-4 inhibitors, GSK-2193874 and HC-067047, was used to determine if specific inhibitors of TRPV-4 have an effect on calcium channels within DRGs in this study.

Chapter 1: Introduction and Literature Review

1.1 General Background/Summary

Cancer stands as the second leading cause of death only behind a variety of cardiovascular diseases.[1] Many researchers and scientists have dedicated their lives to find a cure to this deadly disease; however, only certain treatments have been innovated to decrease the progression or to minimize symptoms of cancer. One specific form of treatment that has shown promising efficacy is the microtubule-stabilizing drug, Taxol, otherwise known as paclitaxel in commercialized branding.[2] This drug has shown results in treatment for lung, breast, and other forms of cancer because of its ability to stop cancer cell division through microtubule stabilization. While there is some proven efficacy, testing has still resulted in certain negative symptoms, such as limited mitotic arrest, acute pain, and chronic inflammation sensations, among others. Specifically, paclitaxel induces peripheral neuropathy, disorders of the nervous system, which inhibits sensorimotor function. In this research paper, paclitaxel induced neuropathy will be investigated and mouse models will be used to try and circumvent the debilitating neuropathy caused by the drug, while maintaining its cancer cell growth inhibiting factors.[2] The focus of this study will center on the initial factors that limit progression in this research in the effect of osmotic pressure and TRPV4 inhibitors on neuronal cultures.

1.2 Nervous System, PNS, and Anatomy of Sensory System

1.2.1 Nervous System

The nervous system is a multi-complex network that allows an organism to transmit sensory and motor signals to and from different parts of the body in order to regulate and coordinate actions throughout it. This system also takes into account surrounding changes in the environment and works in conjunction with the endocrine system to ensure the correct signals are sent and received to provide the correct responses.[3] The nervous system can be thought of as a multi-set up of networks that work together to create a working system to activate or stopping certain reactions according to stimuli. These certain

reactions can go unnoticed in everyday life that control a variety everyday processes, such as feelings, speaking, mechanical actions, memory, among many others. Specifically, the nervous system is comprised of two known main systems, which are the central nervous system (CNS) and the peripheral nervous system (PNS).

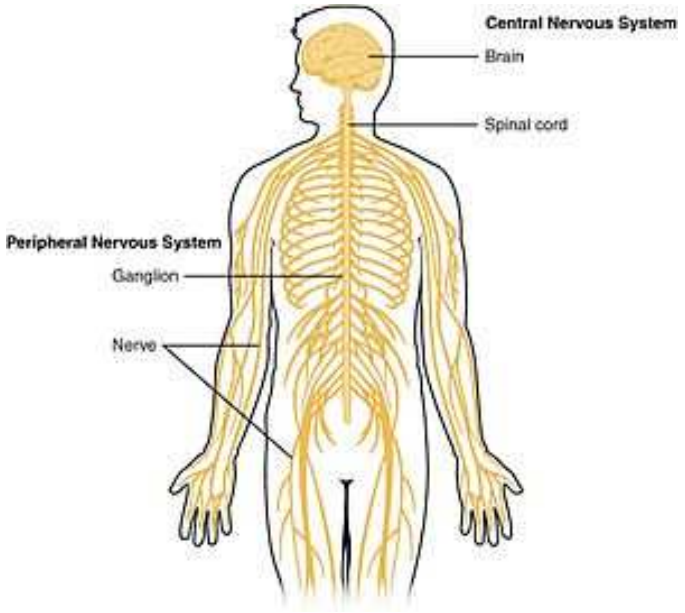

Figure 1.1 **Anatomy of the Central Nervous System.**[4]

1.2.2 Central Nervous System

One of the main systems, the central nervous system is compromised of the brain and the spinal cord. The brain can be separated into four inclusive parts which include: (1) the brainstem, (2) the cerebellum, (3) the hypothalamus and thalamus, and (4) the brain hemispheres.[3] In the head and neck regions, the brainstem contains cranial nerves III-XII which supplies sensory innervation. It is located in the back part of the brain and contains the majority of cranial nerves. Specifically, the brainstem regulates cardiac and respiratory function, like heart rate and breathing. The cerebellum is also located in the back region of the brain and controls motor control. In contrast to the cerebellum controlling motor control and activity, the brainstem controls sensory innervation. Sensory systems of the spinal cord and the other parts of the brain send signals throughout the body in order to control bodily functions. The thalamus and

hypothalamus serve as the bridge between the cerebral hemispheres and the brain stem in order for them to work together. Specifically, the hypothalamus controls pituitary secretions by releasing hormones that inhibit or stimulate the pituitary gland, which regulates an assortment of organs throughout the body. Consequently, the thalamus serves as a middle ground, which sends and receives sensory signals to various cortical areas. Lastly, the cerebral hemispheres contain various structures, including the basal ganglia, hippocampi, amygdalae, and the cerebral cortex. Movement regulation is aided by the basal ganglia. The amygdala processes emotional information from the hypothalamus and is part of the limbic system. Lastly, the cerebral cortex controls certain processing of sensory information and then using these signals to relay motor function.[3]

The spinal cord, which serves as an extension of the brain and CNS, is a main structure in the body. This structure transmits motor signals to the motor cortex while sending sensory signals to the sensory cortex. It consists of many nerves, usually classified as efferent or afferent nerves. Comparatively, efferent nerves send motor signals away from the brain towards the body to cause motor function, while afferent nerves carry nerve signals from sensory stimuli to the brain, both of which are a part of the PNS. The structure is composed of nervous tissue that extends from the brainstem to part of the lumbar vertebrae in the body.[3]

1.2.3 Peripheral Nervous System

While the CNS is made of more dense components, in contrast the PNS is composed of different nerves and ganglia that are responsible for transmitting information to and from the CNS.[5] The PNS can primarily be separated into two divisions, the motor and sensory. Some of the nerves that are a part of the PNS include the sciatic nerve, the radial nerve, and the ulnar nerve; however, the PNS can include any nerve from any part of the body that respond to certain stimuli. Dorsal root ganglion will be the focus of this research paper and will be covered more in depth as the focus of this research paper and modeling.[5]

1.2.4 Sensory Pathways and Pain

The two sections the peripheral nervous system is split up into the somatic nervous system (SNS) and the autonomic nervous system (ANS). Research has shown that the SNS is associated with control of

reflexes and voluntary body movements. In contrast, the ANS acts and occurs functions without conscious control.[5] In more detail, the SNS is composed of spinal and cranial nerves, which control voluntary and involuntary body functions. Spinal nerves are peripheral nerves that relay sensory information to and from the spinal cord, while cranial nerves carry information to and from the brain stem. The pathway nerve signal follows and begins with upper motor neurons within the primary motor cortex and are transmitted down the spinal tract to control voluntary muscles. Once stimulated, signals are sent back and taken in by receptors of lower motor neurons.[6] The ANS focuses on regulating basic bodily functions such as digestion and breathing. The primary purpose of the ANS is to maintain homeostasis through system divisions that comprise the ANS, which are the sympathetic and parasympathetic divisions. These two divisions react to specifically activate or inhibit a response formed from each other. Different than the SNS, most autonomous functions are involuntary but can work in conjunction with the SNS to provide voluntary control.[6]

The sensation of pain comes with the activation of certain receptors within afferent pathways. Pain pathways start with pain sensitivity, which lead into a response of signals sent to the spinal cord from the peripheral nervous system. This step of the pathway leads these signals to the central nervous system to provide a response from these signals.[6] This primary mechanism can be broken down into three steps: transduction, transmission, and modulation. Transduction converts stimuli events into chemical tissue responses, which is followed by conversion of this into electrical signals in the neurons. Finally, it is transduced back into chemical events within the synapses. Then, transmission takes place right after which relays the electrical signals from the post-synaptic terminal of a cell to the pre-synaptic terminal of another. Modulation come as the last step, and occurs throughout to control and adjust responses at all levels of nociceptive pathways. Once these three events are gone through, the pathway of pain allows us to feel the pain sensation caused by the harmful stimuli.[6]

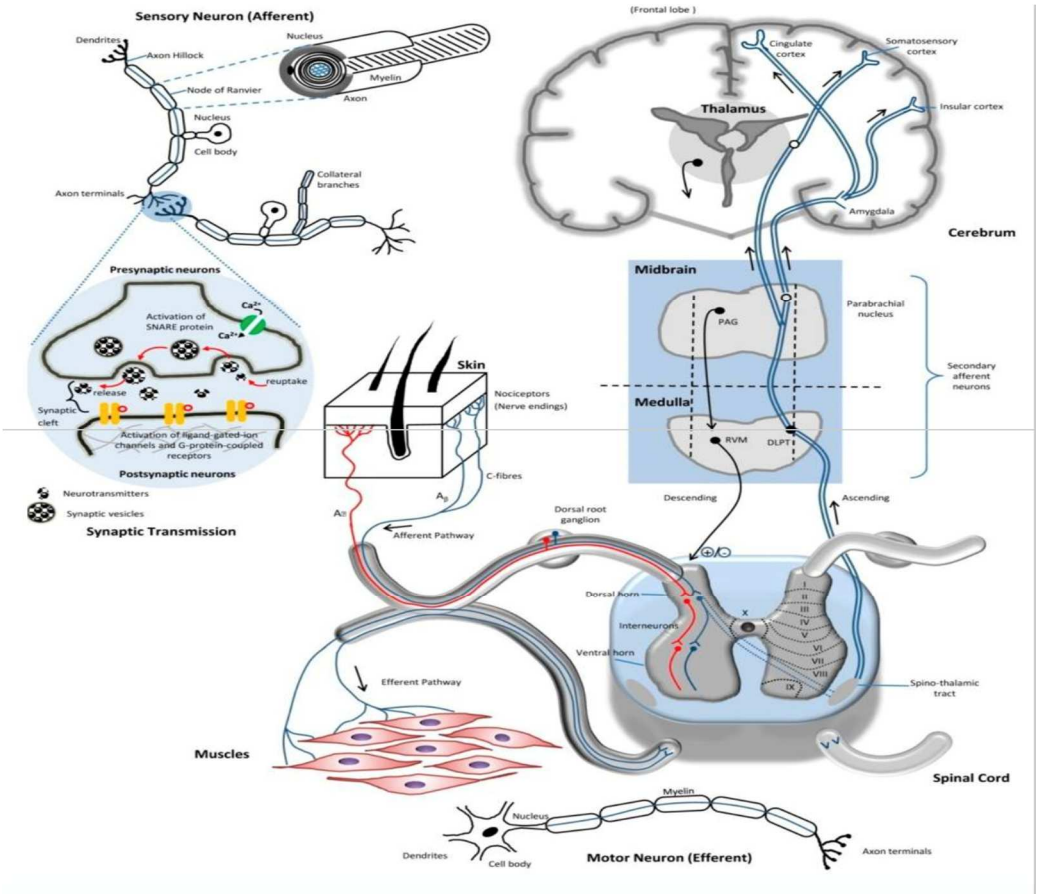

Figure 1.2 **Processes of Sensory Pathways and Pain.**[6]

1.2.5 Neurons and Nerve Endings

Neurons are cells that are electrically excitable to send, receive, and transmit information throughout the body through electrical and chemical signals.[7] These signals are communicated through neurons through bridges called synapses. Because of this, neurons connect and form a neural circuit, which are used throughout the body. The three broad and majorly known types of neurons are sensory neurons, motor neurons, and interneurons.[7] Sensory neurons respond to stimuli of all sorts whose signals are converted via transduction. Conversely, motor neurons receive signals from the spinal cord and brain to control motor function. Separate from sensory and motor neuron functions, interneurons connect neurons to other neurons to form a sort of neuron bridge. Anatomically, neurons are made up of a cell body, axons, and dendrites. The soma or cell body is the bulbous part of the neuron, which contains the

cell nucleus, in which dendrites branch off of. Dendrites are thin structures that branch off in multiple areas forming a structure called the dendrite tree. Axons are upstream neurons, which transmit electrical signals onto these dendrites, which regulate the action potentials produced by the neurons.[7]

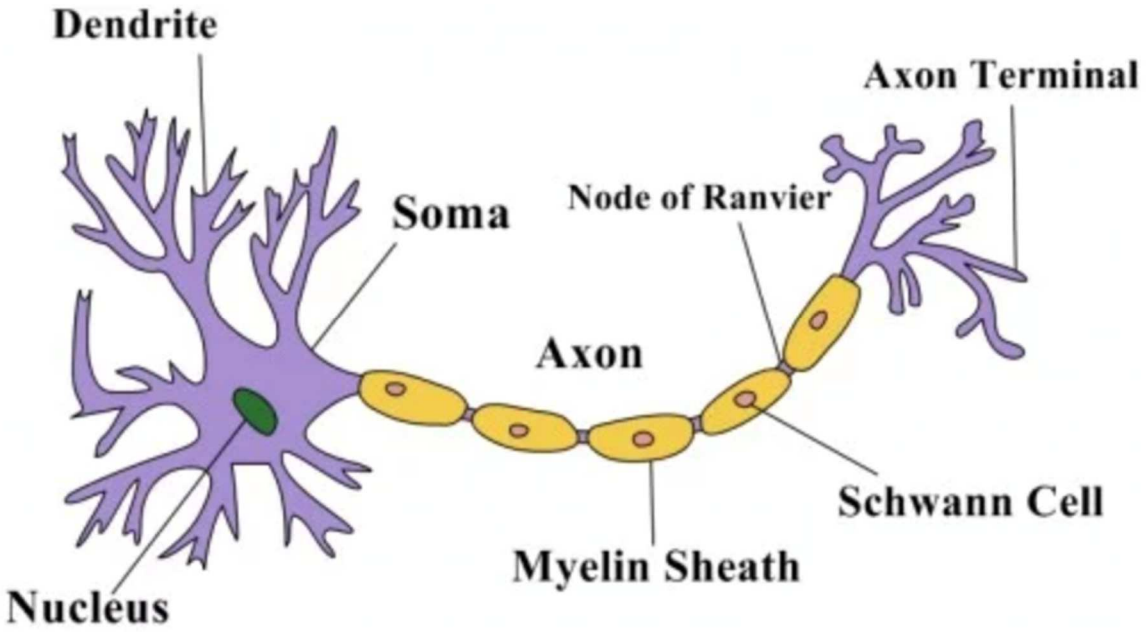

Figure 1.3 **Anatomy of Neuron.**[8]

1.2.6 Dorsal Root Ganglia

The dorsal root ganglion (DRG) is a cluster of neurons that are part of the spinal nerves located in the spinal cord.[8] In the spinal cord, these ganglions are located between the spinal nerve and the dorsal root and contain pseudo-unipolar neurons that send and receive signals to and from the CNS and PNS. Because these neurons are involved in relaying information in response to stimuli, these neuron clusters become an important target for research and potential source of treatment due to signaling responses that occur during inflammation or injury.[9] Because of this, there are many uses to using DRGs in research whether to minimize its properties or to stimulate the clusters to achieve certain responses. Structurally, the DRG lacks a protective membrane, which contributes to its permeable tissue properties, making it useful for drug delivery. In addition because of this permeability, this tissue has a high density of blood

capillaries forming a rich blood supply. This aids in research purposes, because the toxic concentration threshold is a lot higher due to these high perfusion rates and produces more efficient results in all. Damage to the nerve also causes responses in the system, which can be seen through increased expression of the calcium channel, the sodium channel, and transient receptors. Specifically, the dorsal root nerve lowers the voltage threshold needed to fire action potentials that are needed to send signals. This property occurs during a mechanical stimulus from either within or the environment.[9] Because of these attributes, DRGs will be used in order to conduct the studies of this paper.

1.3 Cancer and Chemotherapy

1.3.1 Cancer

Cancer is a group of diseases varying from body part to body part causing abnormal cell growth within the body. Because of this, there are more than a hundred different distinct types of cancer.[10] This starts when a cell starts its own process of proliferation causing abnormal cell growths or neoplasia. When neoplasia forms a mass of cells, and these are called tumors. According to research, there are two main types of tumors, benign and malignant tumors.[10] Benign tumors lack the ability to invade neighboring tissue and are confined to its original location. Because of this when removed these do not usually grow back and are more treatable than malignant tumors. In contrast, malignant tumors sometimes do and have a faster growth rate than benign tumors. However, most importantly these can spread throughout the body through the lymphatic or circulatory system.[10] Most main types of cancers fall into three groups. Sarcomas are the most rare of the three types of tumors that are caused in connective tissue, such as bone, skin, muscle, etc. Leukemia and lymphomas account for approximately 8% of malignant tumors, coming from the immune system and circulating blood forming cells. Carcinomas are the main type of cancer, which target epithelial cells, and account for about 90% of human cancer.[10]

There are six widely known constituted traits that define the evolvement of cancer.[11] These six all contribute to the instability of a cell before leading to abnormal cell growth: apoptosis, inducing angiogenesis, starting replicative immortality, denying growth suppressors, sustaining proliferative

signaling, and allowing metastasis, and invasion. In addition to these six, two more have recently been ascertained in research which are tumors promoting inflammations and genomic mutations.[11]

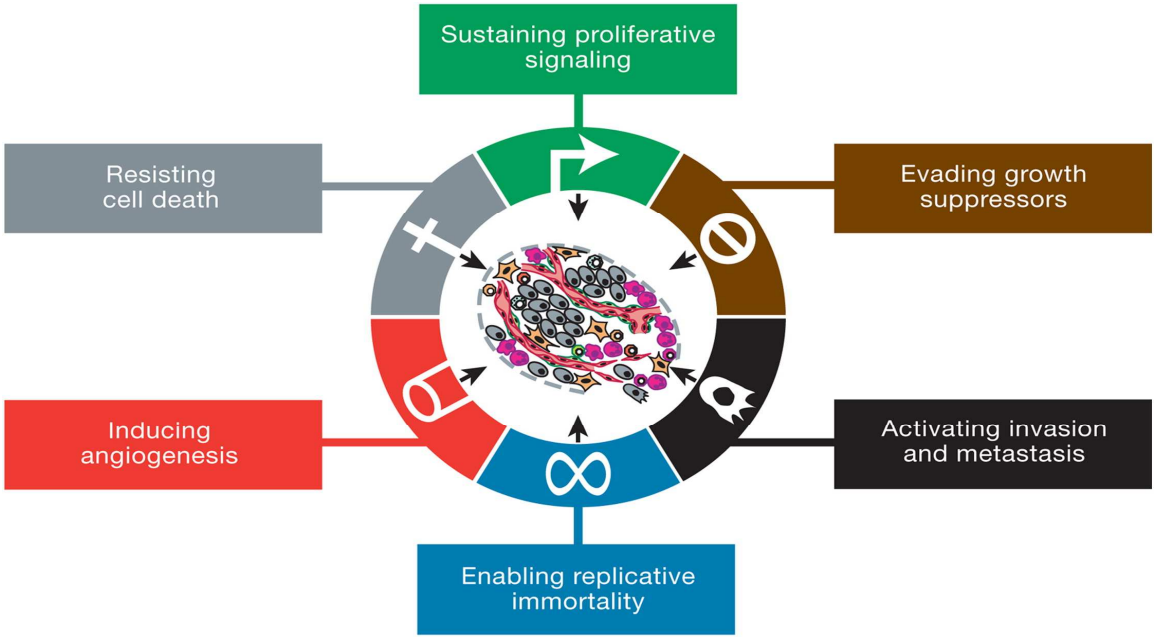

Figure 1.4 **The Six Progressions of Cancer.**[11]

While there have been many promising steps in the frontier of cancer, only alternative treatments to extend length and quality of life of patients with cancer have been recorded.[11] Many characteristics of cancer have been determined, which has allowed scientists to delve into significant research of its potential possible treatment but there is still a long way to go to fully treat the disease.

1.3.2 Treatments

While cancer cells can be excised surgically or eliminated through different types of radiation or chemicals, it has been an ongoing problem to be able to get rid of every cancer cell.[10] Because malignant tumors can alter the cell growth process and proliferate to an absurd degree, leaving behind a few cancerous cells can lead to the resurgence of the disease. In addition, cancer cells are able to adapt and evolve a resistance to many chemicals found that have efficacy and are used to treat it. This is in part due to its mutability, which amplifies part of the genome that contains gene *Mdr1*.[11] Amplification of this gene increases plasma membrane bound transport, which prevents the accumulation of drugs from

treatment by pumping them out of the cell. Furthermore, cancer cells have a selective advantage to amplify all sorts of different genes, which will help it survive. Current treatment focuses on the loss of genetic instability and the loss of cell-cycle control processes.[11] Because of this, traditional therapy relies on drugs and radiation to eliminate cancer cells before they are able to multiply and evolve. Future treatment focuses on more selective ways to get rid of cancer cells in order to avoid symptoms. Because killing off cancer cells introduces harmful chemicals into the body, more extreme routes for treatment prove to have no efficacy due to negative side effects and difficulty of applying these treatments. In order to circumvent these obstacles, cancer treatment has a wide range of targets that are tested in addition to an assortment of drugs that will eliminate cancer cells as a whole. However, another promising treatment is to not directly target the cancer cells to avoid toxicity but to cut off its blood supply needed to reproduce in the body.[10] Understanding cancer biology has come a long way, but finding a cure is nevertheless an ongoing search.

One standardized form of treatment that studies have proven to have some sort of efficacy is chemotherapy. Chemotherapy has potential curative possibilities but also aims to prolong life through reduction of symptoms of cancer. This form of treatment focuses on using certain agents and chemicals that are cytotoxic that interferes with cell division.[11] One certain type of drug that has shown efficacy is platinum based which is used for around 50 percent of chemotherapy treatments among patients. Dosage is determined by body size in order to optimize drug exposure and treatment outcomes for each specific patient. While chemotherapy has certain positive effects, there are also common side effects such as myelo-suppresion, hair loss, and damaging cells that rely on dividing rapidly. Currently, this targeted therapy has been researched in order to minimize symptoms as well as amplify efficacy to kill tumors and reduce toxicity. The second major form of treatment is radiation therapy, which focuses on using ionizing radiation to kill and contain cancer cells.[11] Different than chemotherapy, radiation therapy allows for localization of the treatment but also can be used on adjacent areas to prevent tumor spreading and reformation. The treatment is primarily painless and there are minimal side effects; however, this depends on the treatment itself as well as the patient. Some side effects from this include skin irritation and

fatigue, along with some other broad range of acute side effects. The major negative side effect of radiation comes from long-term exposure that would affect a patient in the future, such as fibrosis, hair loss, and even potentially the reoccurrence of cancer.[12]

1.3.3 Paclitaxel

Taxol, better known as the brand Paclitaxel (PTX), is a microtubule-stabilizing drug approved by the Food and Drug Administration for the treatment for a variation of forms of cancer. However, many preclinical trials and clinical trials were gone through in order to prove the efficacy and sustainability of the drug.[2]

In the mid 1900s, the National Cancer Institute and the U.S. Department of Agriculture worked together on a plant-screening program to test the extracts of the plants in order to screen for anticancer activity. Eventually, certain extract from the bark of *T. brevifolia* showed promise was found to be cytotoxic, and entered the drug development program for further research.[2] This in turn led to a high demand of taxol for the increased amount of preclinical trials that wanted to test the extract for its anticancer properties and potential as a treatment for cancer. However problems occurred due to removing the bark from the tree killed the trees, which making *T. brevifolia* endangered. Due to these recurring demands and quantity of taxol, this caused laboratories to set out to develop a complete synthesis of the extract, which was eventually successful in the late 1900s. Taxol became commercialized and eventually was renamed to paclitaxel as a commercialized generic brand name.[2]

PTX promotes the connection and assembly of microtubules by reducing the concentration of purified tubulin subunits needed for polymerization. In turn, this increases the amount of tubulin subunit formation. In specificity to cancer, PTX provides substantial antitumor traits due to its property to arrest cells in the metaphase. The presence of unattached kinetochores due to PTX arrests cells in mitosis, which could possibly be used in the research and treatment of cancer. In addition, PTX treatment reduces tension on the kinetochores to maintain bipolar connections, which is useful in halting cells in mitosis.[2]

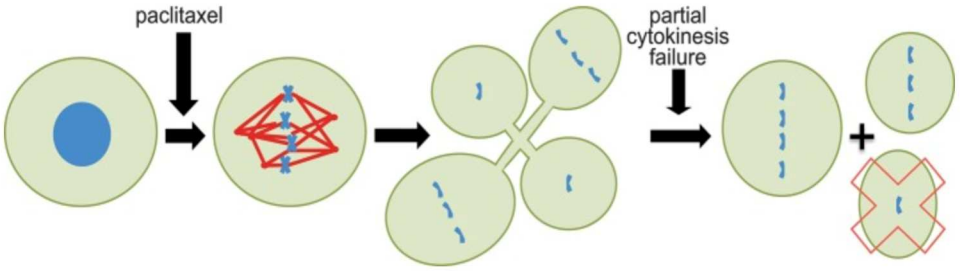

Figure 1.5 **Effect of Paclitaxel.**[2]

1.4 TRPV-1 and TRPV-4 Mechanical Channels

1.4.1 TRPV-1

Transient receptor protein cation channel subfamily V member 1, TRPV-1, is a protein that is encoded by the TRPV-1 gene.[13] This receptor is also known as the capsaicin or vanilloid receptor 1 and works to detect and regulate body temperature. This channel can be activated or deactivated through physical and chemical stimuli. Capsaicin is one of the best-known activator of TRPV1, which is a special compound in chili peppers, along with any other sort of environmental stimuli or compound that increases temperature.[13]Activating TRPV1 leads to a burning sensation in the body, which causes inflammation and tissue harm. This initial sensitization to stimuli does not remain stagnant, as prolonged exposure to stimuli leads to desensitization in which extracellular calcium ions are released to control the effect. Due to its properties, TRPV-1 is a focused target for the treatment of pain, especially in the PNS. The two clinical ways the TRPV-1 channel is through blocking TRPV-1 channel to reduce pain, but also through activating TRPV-1 in order to relieve pain through desensitization. As such there is much research in regulating TRPV-1 channels. In DRGs, there is expression of an ion channel that can be activated by capsaicin making DRGs and TRPV-1 important factors in scientific research.[13]

1.4.2 TRPV-4

TRPV-4 is member 4 of the transient receptor potential cation channels similar to TRPV-1.[13] While TRPV-1 channels are activated through temperature change; TRPV-4 channels are activated through primarily mechanical signals, but also in some degree thermal changes.[14] These channels are

gated by tension, which is affected by these mechanical signals. As these signals can cause stretch or stress to the membrane or cytoskeleton, these potentially activate or deactivate the channels. The TRPV-4 encoded protein is also a calcium permeable cation channel, and has importance in many physiological diseases that impair motor function. Similar to TRPV-1, deactivation and activation of these channels has significant impact on scientific research to up-regulate and de-regulate certain functions throughout the body.[14]

1.4.3 TRPV-4 Inhibitor Differences

The two specific inhibitors to be tested in this study were HC-067047 and GSK-2193874. Both inhibitors are both potent and selective TRPV-4 antagonists.[15,16] Both can inhibit TRPV-4 activation by various stimuli, including osmotic stimulation and temperature changes. HC-067047 has high selectivity, which makes it a promising candidate for a TRPV-4 inhibitor.[15] It has a 471.51 molecular weight compared to 691.62 of GSK-2193874.[17,18] GSK-2193874 has an IC_{50} of 40nM compared to HC-067047's IC_{50} of 17nM.[17,18] IC_{50} means the concentration of the inhibitor that causes binding to be reduced by 50%. Both can be involved in TRPV-4 regulation in which there is interplay between arachidonic acid binding sites and the rearrangement of phosphorylation-induced formations of the C-terminal helix.[19] They both bind to the C-terminal calmodulin-binding site.[15] Calmodulin serves are signal transducers that connect cell stimuli to certain cell functions. This means that calmodulin regulates TRPV-4 channels by binding to these C-terminal calmodulin-binding sites.[19] With the introduction of inhibitors to this, this causes these inhibitors to bind to these sites and limit TRPV-4 activity. This is done by maximizing the inhibitory concentration (IC) to its full potency to cause this binding.[15] For GSK-2193874, it inhibits the activation of recombinant TRPV-4 currents when applied to an extracellular solution in cells expressing native and recombinant TRPV-4.[17] HC-067047 inhibitors inhibit hERG channel and the menthol receptor TRPM8.[18] Studies have shown that both these inhibitors are potent, and specific antagonists.[15,16] Both have no known affects on other channels.

1.5 Peripheral Neuropathy

1.5.1 Peripheral Neuropathy

Peripheral neuropathies are disorders that affect the peripheral nervous system and impair sensorimotor function.[20] These disorders can be classified by the site and properties of sensory symptoms that are a consequence of disease of the nerve itself or through a systemic illness. Some symptoms include paresthesia, numbness, and weakness. Peripheral neuropathies have a broad range of area that it affects, some which cause chronic development of pain, while others could have respiratory insufficiency depending on the localization.[20] Because of this, localization of the neuropathy highly contributes to proper diagnosis and treatment and is the focus research in this field.[14] As of now, certain treatment approaches include but are not limited to trying to reverse the pathophysiological process, stimulation of nerve metabolism, and symptomatic therapy to alleviate symptoms.[21]

1.6 Microtubules and Tau

1.6.1 Microtubules

Microtubules are a construct of tubulin heterodimers that polymerize into proto-filaments.[7] These tubules are highly dynamic and are involved in a number of cellular processes such as maintaining the structure of the cell. These processes play a crucial role in cell function such as cell division, morphology, and transport. The microtubules are constructed with cilia and flagella, which provide groundwork for intracellular transport including the movement of vesicles. Because it is involved in the transport of vesicles and organelles, the cellular cytoskeleton can also influence gene expression. The trait contributes substantially to targets of potential cancer treatments that involve the alteration of gene expression.[7]

1.6.2 Tau

Tau is a microtubule-associated protein that is frequent in neurons of the CNS, which attaches to the interface between tubulin heterodimers.[22] Typically, Tau is not present in dendrites and is presently active only in the distal locations of axons. This protein promotes the creation and assembly of microtubules, stabilization, and influences neurite outgrowth. Previous studies have shown that Tau plays

an important role in the pathology of many neurodegenerative diseases.[22] By affecting the Tau-microtubule complex, these neurodegenerative diseases typically will cause Tau detachment and in turn interrupt axonal transport. Tau controls microtubule stability through different isoforms and phosphorylation.[22] In the body, there are six different tau isoforms that exist in brain tissue and each are defined by the number of binding domains each have.[20] The more binding domains there are corresponds to the efficiency that the isoform is at stabilizing microtubules. When Tau is phosphorylated, microtubule organization is interrupted, but is still dependent on the development stage of each particular case. As Tau plays a part in many neurodegenerative diseases, the protein has come into focus in many studies as to increase or limit its properties, in order to find treatment for these diseases.[23]

1.7 Calcium Dynamics and Modeling

Calcium acts as a messenger in primary sensory neurons. Consequently, in dorsal root ganglion, which plays a role in nociception, this is exemplified by disrupted calcium signaling.[24] This could be a response that increases calcium flow throw channels leading to hypersensitivity. The downstream effects of calcium regulate an assortment of events such as gene expression, excitability, neuronal differentiation, and more.[24] The immediate decrease or increase of these calcium levels is based on membrane depolarization and are caused by influxes through the membrane, in which the focus for this study is the effects of osmotic pressure due to the importance of mechanical loading effects on the cell membrane.[25] Introducing osmotic pressure to our specific system of dorsal root ganglion cells theoretically should increase the amount of calcium influx by the activation of TRPV-4 channels, which are mechanically regulated.[25] With water flow through TRPV channels, this causes the cell to swell in due part due to hypo-tonicity.[25] As increased membrane tension activate the TRPV-4 channels, this opening allows for calcium ions to travel through.[26] Calcium rushing in is caused because there is more calcium

outside the cell than there is inside by following its gradient through the calcium channel. Over time, the cell structure should return to homeostasis in which there is a restoration of calcium levels and a reduction of swelling. This is due to BK_{Ca} channels, which respond to elevated levels of intracellular calcium levels.[26] However, TRPV-4 channels may not be the one channels of the membrane affected as previous studies have shown there are other certain channels in dorsal root ganglion cells such as the piezzo and pannexin channels.[27,28]

In the overall picture, introducing paclitaxel to dorsal root ganglion neurons leads to an increased expression of low-voltage activated calcium channels, which leads to a greater influx of calcium that leads to hypersensitivity.[29] Previous studies have shown that there is increased spontaneous activity and calcium channel activity in dorsal root ganglion and spinal cord segments when these were treated with paclitaxel.[29]

Chapter 2: Materials and Methods

2.1 Dissections and Harvesting

The mice used in this study are purely wild-type mice (WT) to test for baseline and fundamental interactions with osmotic pressure and TRPV-4 inhibitors for further studies on this topic. The dorsal root ganglia (DRG) of these wild-type mice will be extracted in a step-by-step protocol.[30]

The targeted WT mouse will be euthanized through carbon dioxide inhalation. Death by carbon dioxide will be induced as quickly and as painlessly as possible. In such, death will be confirmed through cervical dislocation. The procedure to harvest the DRGs will start by placing the mouse on a blue pad, dorsal side up. Using surgical scissors, the head of the mouse is removed where the superficial sphincter muscle of the neck lies. The forelimbs can be kept attached for orientation.

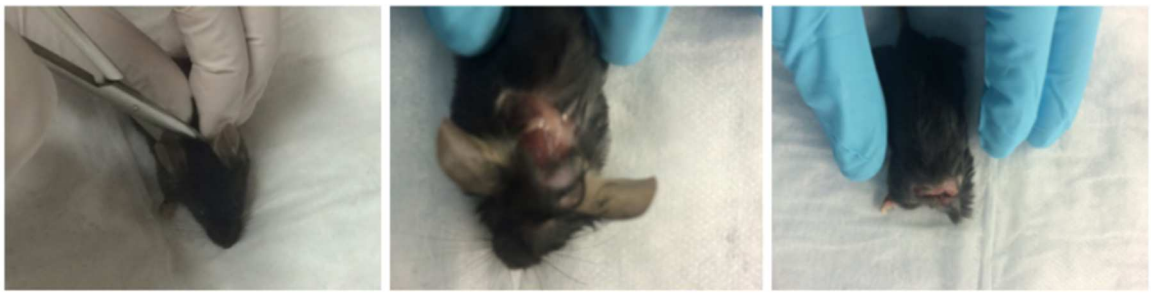

Figure 2.1 **Start of Dissection Protocol.** Cutting the mouse dorsal side up to remove the head.

The skin is separated from the muscle layer through the use of surgical scissors cutting down along the spine rostral to caudal in order to create an I shape. The skin should be slightly peeled to the side to expose the organs and thoracic cage. Flipping the mouse to the ventral side and starting from the caudal end, gently remove all the organs with the least amount of damaging or disruption to the spine. Forceps can be used in order to find points to anchor for cleaner organ removal. Once organs are removed, continue cutting along the sides of the thoracic cage vertically from the armpit to the hip to remove any excess tissue or organs.

Figure 2.2 **Removing All Excess Organs.** The mouse is dissected in order to expose the spinal cord while leaving the limbs intact for orientation.

Keeping the mouse on the dorsal side, small spring scissors are used to cut the spinous process of the spine by inserting the scissors between the spinal cord and the tissue layer of the spine through the spinal canal from T1 to L5. This step should be taken with precaution as the spine would lose orientation

and the DRGs can be detached from the spinal cord. Using forceps, the vertebral arch of the vertebrate can be spread open to expose the spinal cord.

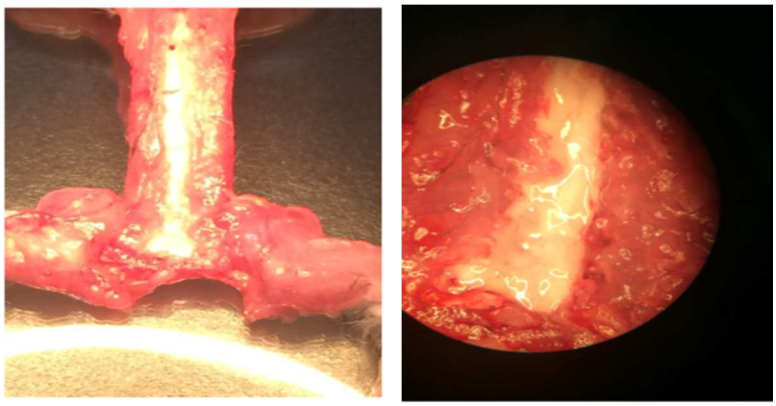

Figure 2.3 **Cutting Open the Spinal Cord.** Cut open the spinal cord from T1 to L5 to expose the tissue layer of the spine.

Through a microscope, the spinal cord is gently lifted with thin forceps to observe the dorsal roots branching from the spinal cord. Next, cut away at the transverse process connecting the DRG to the spinal cord. The DRG should still be connected to the dorsal root that connected it to the spinal cord. The DRGs are identified by its circular bulb shape and dark speckles. The last step is to place the DRG into a petri dish filled with Neurobasal-A media.

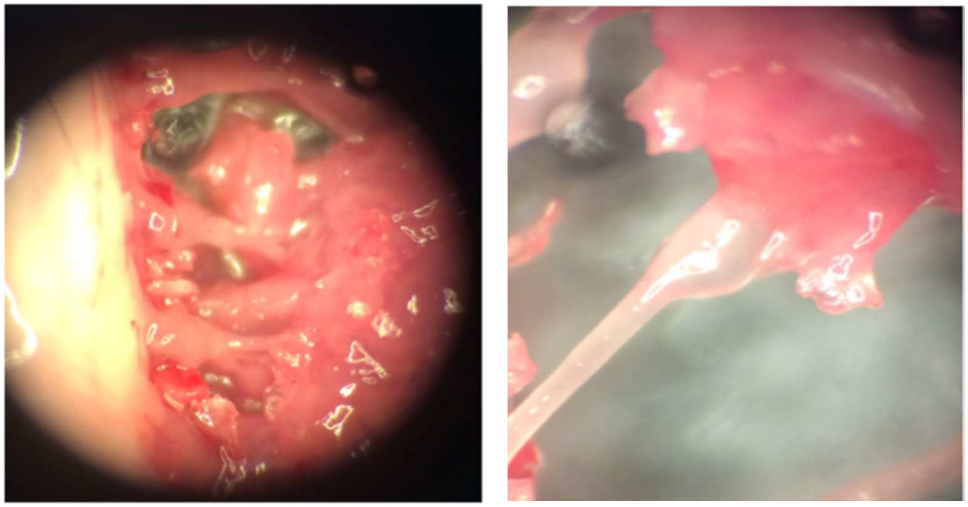

Figure 2.4 **Exposing the DRG.** Using a microscope look into the spinal cord to reveal the DRGs. The DRGs have a circular bulb shape and speckles with a dorsal root attaching it to the spinal cord.

2.2 Dissociation Protocol

The mice DRG harvested in this study will be used in a dissociation protocol to differentiate neuronal cultures to be used in analysis and further discussion.

The protocol is listed as follows. The materials needed for DRG dissociation are HBSS salt solution, Fetal Bovine Serum (FBS), 0.25% Trypsin, and DRG Neurobasal-A media. The dissociation media is with extra ingredients to help promote health of the cell culture. These include 10mL of B27 supplement, 50mL of FBS, 5,000 µL of L-Glutamine, 5 µL of nerve growth factor (NGF) supplement, 5,000 µL of Pen-Strep, and 430 mL of Neurobasal-A media. The initial materials are placed in a 37 degree Celsius water bath for 20 minutes to be warmed up before dissociation. Instead of placing the DRGs in Neurobasal-A media, the harvested DRGS is placed in HBSS. Next these are transferred into a 15mL conical of HBSS and centrifuged at 1000rpm for 1 minute. The HBSS is then to be removed and replaced with 5mL of 0.25% Trypsin. Using a glass homogenizer, the cells are pinned to the wall and bottoms of the conical to homogenize the cells. The conical is placed in the water bath for 20 minutes to digest the tissue. Once removed from the water bath, the conical is centrifuged again at 1000rpm for 1 minute. The Trypsin is then removed from the tissue and washed with 5mL of FBS for 2 minutes, which helps deactivates the enzymes. Next, the FBS is removed from the conical and replaced with Neurobasal-A media and triturated with a glass Pasteur pipette about 30 times. The solution is run through a 70-micron cell strainer and into a 50mL conical tube and then spun in a centrifuge at 1500rpm for 5 minutes. The last step is to re-suspend the solution into plates pre-coated with both mouse Laminin and matrigel to be incubated for 7-10 days for cell growth.

2.3 Imaging and Data Analysis

Once cell growth is confirmed, plates are prepped for calcium imaging via confocal microscope. This is done by removing the plating media and re-suspending the cells with a solution composed of 5mL of basic Neurobasal-A media, 50 µL of PowerLoad, and 5 µL of Fluo-4 dye. These components come from a Fluo-4 Calcium Imaging Kit. Once incubated for 20 minutes with the solution, the plates are

washed with HBSS or plain Neurobasal-A media. The plates are then ready to be imaged through confocal microscopy. Videos of three minutes in length are taken once cells are located and transferred to ImageJ for further analysis. Data for integrated density and area are taken from these videos for each particular cell and exported to MatLab and Excel for graphing analytics. Integrated density is taken as the sum of pixels in the cell selected. These graphs are plotted by integrated density versus time with baseline and experimental variable graphs plotted conjunctively in Excel. Next, these graphs were also plotted in MatLab to form trend lines. Data taken from these graphs and videos are then taken for analysis and results.

2.4 Osmotic and Inhibitor Experiments

After locating a set of cells, three minute videos are taken as a baseline for each plate during calcium imaging. Experimental groups of 5 cells in each group for osmotic testing include taking data for media and water. Media was set at 25% to be added to each plate imaged in 0.5mL syringes. Water osmotic tests were done in sets of 10%, 25%, and 50% of the amount of media residing in each plate concurrently (equivalent to 0.10 mL, 0.25mL, and 0.5mL). The same set of cells was located again for each test once the variable was added to ensure consistency between the baseline and the experiment; all experiments done are recorded in three minute videos.

For inhibitor experiments, HC-067047; >98% (HPLC) and GSK-2193874; >98% (HPLC) which are both specific, potent antagonists and inhibitors of TRPV-4 ion channels are used. These two compounds come in powder form and are solubilized with dimethylsulfoxide (DMSO). For HC-067047 and GSK-2193874, 1.06 mL and 722.94 µL of DMSO was added to 5mg of each compound respectively to solubilize to create a 10mM solution. This 10mM product is then added to 0.995mL and 0.9995mL of media for dilution to create a 5µM concentration of inhibitor. The experiments are done by changing out the process of re-suspending the plates in media after calcium imaging preparation with this dilution solution created with inhibitors. The plates are then incubated for an additional 45 minutes to be absorbed into the cells.[31] Three minute baseline videos are taken with these plates again prior to adding variable to

the experiments. Each experiment was tested with 5 different cells from multiple plates. Following these baseline measurements, 25% of media and 25% of water is added for each variable test. Three minute videos of these are taken of the same cells located for the baseline. Data from this is taken for analysis as such in osmotic testing.

To see the effect of inhibitors over time on DRG cells, imaging was taken after the addition of HC-067047 and GSK-2193874 in separate experiments at time points 0 minutes (baseline), 20 minutes, and 45 minutes. Each of these experiments was tested on 5 different cells at the varying time points to see the effect of inhibitors on the cells over time. These inhibitors were added after the baseline.

In both osmotic and inhibitor experiments, post/pre ratio was taken by dividing the maximum integrated density value from variable (water, media, and inhibitor) experiments by the minimum integrated density value of baseline testing. For timed inhibitor experiments, the calculation remains the same, but data imaged at 20 minutes and 45 minutes were separately calculated to the baseline cells were imaged.

2.5 Statistical Analysis

To perform statistical analysis, results taken from osmotic and inhibitor experiments were run through Excel and StatPlus. This program was meant to create p-values for groups of data sets to see if there is a significance of an effect from the factors inputted. In this study, this is done through an analysis of variance test (ANOVA) in order to test this. In a one-way ANOVA test, which only has one factor, it proves the experiment has a significant effect based on the variable changes. This is done on osmotic experiments, as there is only a change in the amount of water inputted into the system. This is also done for the post/pre ratio values as well as both pre-60s and post-60s experimental decay constants. This one-way ANOVA test was also done for the timed inhibitor experiments, where the only factor was time. A two-way ANOVA test is done on inhibitor experiments, as there is more than one factor. This test takes into account two factors, and tests if there is an effect of factor 1, factor 2, and if there is an interaction of factor 1 and 2 on the results. This is done for inhibitor experiments for post/pre ratios separately for each

inhibitor with the factors being whether or not there is an inhibitor involved, as well as if there is water or media added back into the system after incubation. For both types of test, if there is a value less than 0.05 for the p-value, the data illustrates that there is an effect of whichever factor is being tested. However, while these tests shows if there is an effect or not, it is unable to specifically identify what the effect is. Post-hoc comparison tests were done after these ANOVA tests to test for significance between the variables within the study.

Chapter 3: Results

3.1 Osmotic Testing

3.1.1 Osmotic Results

Integrated Density was taken versus time to produce graphs for each experiment. In media, baseline and post-media addition both had similar decays for each of the 5 cells. After the addition of media, the integrated density minimum of baseline matched the maximum integrated density of media resulting in no jump in integrated density (Figure S_1). Adding 10% water resulted in a similar trend to media; however, a majority of the cells for 10% experiments had a drop off between the baseline and post-water addition values (Figure S_2). Adding 25% water or 50% water resulted in a jump in integrated density beyond the minimum integrated density of each baseline taken for each cell respectively (Figure S_3, S_4).

Post/Pre ratio means were taken cumulatively of the 5 cells for each experiment and plotted on a bar graph with standard error of mean bars (Figure 3.1). Media and 10% water experiments demonstrated the same trend as shown in the analytical plots, hovering at around a value of 1 ratio. 25% and 50% water experiments both approximated at around a value of 1.4. Normalized integrated density was also plotted to account for area in these figures as well (Figure S_1, S_2, S_3, S_4).

The values of minimum intensity, maximum intensity, and the post/pre ratio of each cell in these experiments are shown in Table 3.1, representing what was shown in Figure 3.1.

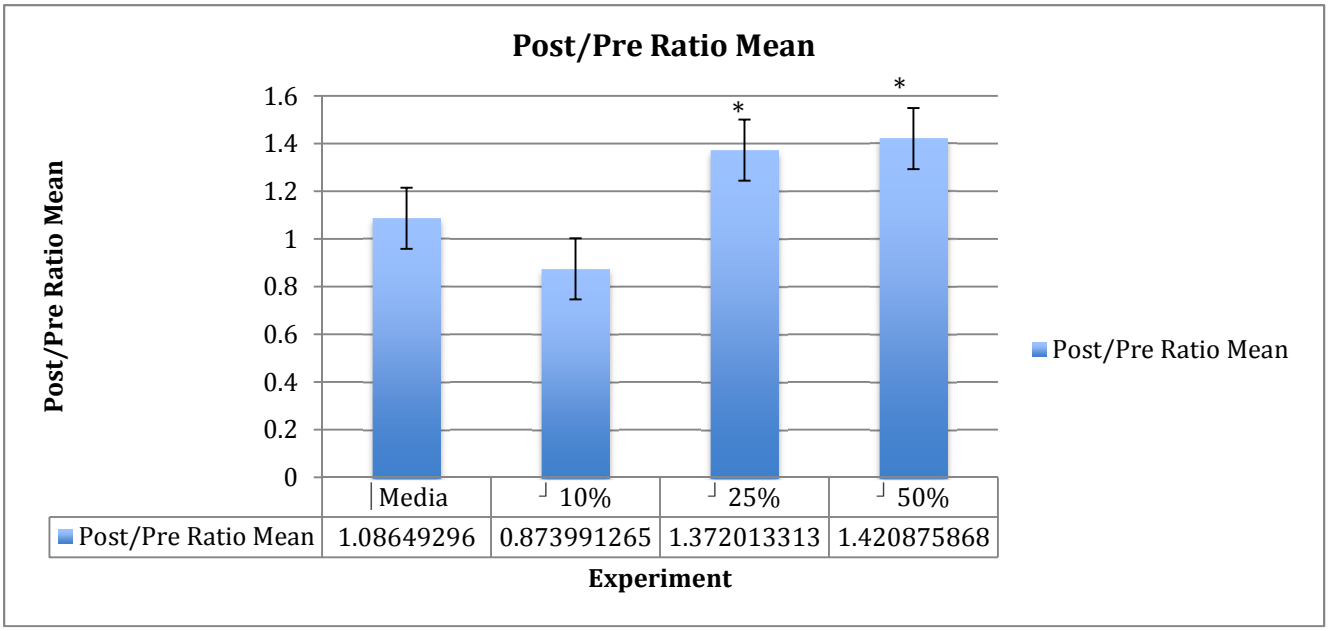

Figure 3.1 **Osmotic Post/Pre Ratio Means**. Media, 10% water, 25% water, and 50% water experiments resulted in a post/pre ratio mean of 1.086, 0.874, 1.372, and 1.421 respectively. *Post-hoc comparison showed significant difference between these experiments and 10% water experiments.

Table 3.1 **Osmotic Results of Each Cell.**

Cell Number	Experimental Group	Minimum Intensity (Pre)	Maximum Intensity (Post)	Post/Pre Ratio
1	Media	28625	33425	1.16768559
2	Media	82339	71088	0.863357583
3	Media	82339	74636	0.906447734
4	Media	24765	34773	1.404118716
5	Media	168620	183940	1.090855177
1	Water 10%	133790	97323	0.727431049
2	Water 10%	66355	53765	0.810262979
3	Water 10%	65386	65451	1.000994097
4	Water 10%	33711	29014	0.860668624
5	Water 10%	103740	100690	0.970599576
1	Water 25%	11769	16755	1.423655366
2	Water 25%	147200	182340	1.238722826
3	Water 25%	150370	175230	1.16532553
4	Water 25%	146890	184280	1.254544217
5	Water 25%	59843	106390	1.777818625
1	Water 50%	82494	92730	1.124081751
2	Water 50%	72862	113720	1.560758695
3	Water 50%	50756	102670	2.022815037
4	Water 50%	39646	51308	1.294153256
5	Water 50	78892	86984	1.102570603

3.1.2 Osmotic Trend Line Results

Trend lines for each graph were plotted to see the overall trend of each experiment. Initially, both linear and exponential lines were fitted to see which would be best for the results received (Figure S_5, S_6, S_7, S_8). These trend lines both seemed fitting for the plots achieved for osmotic testing; however, as some exponential trend lines did not fit properly on all cell experiments, it was deemed better to use two linear fittings. The two linear fittings were used for the first 60 seconds, which seemed to be where the initial drop-off ended, and for that point onwards to 160 seconds (Figure S_9, S_{10}, S_{11}, S_{12}). Then it was decided because of this that this form of trend lines would be used for inhibitor experiments later on in the study. For all cells in each experiment, there was an average decay in trend lines over the complete 3 minutes (Figure 3.2). These values are listed in Table 3.2.

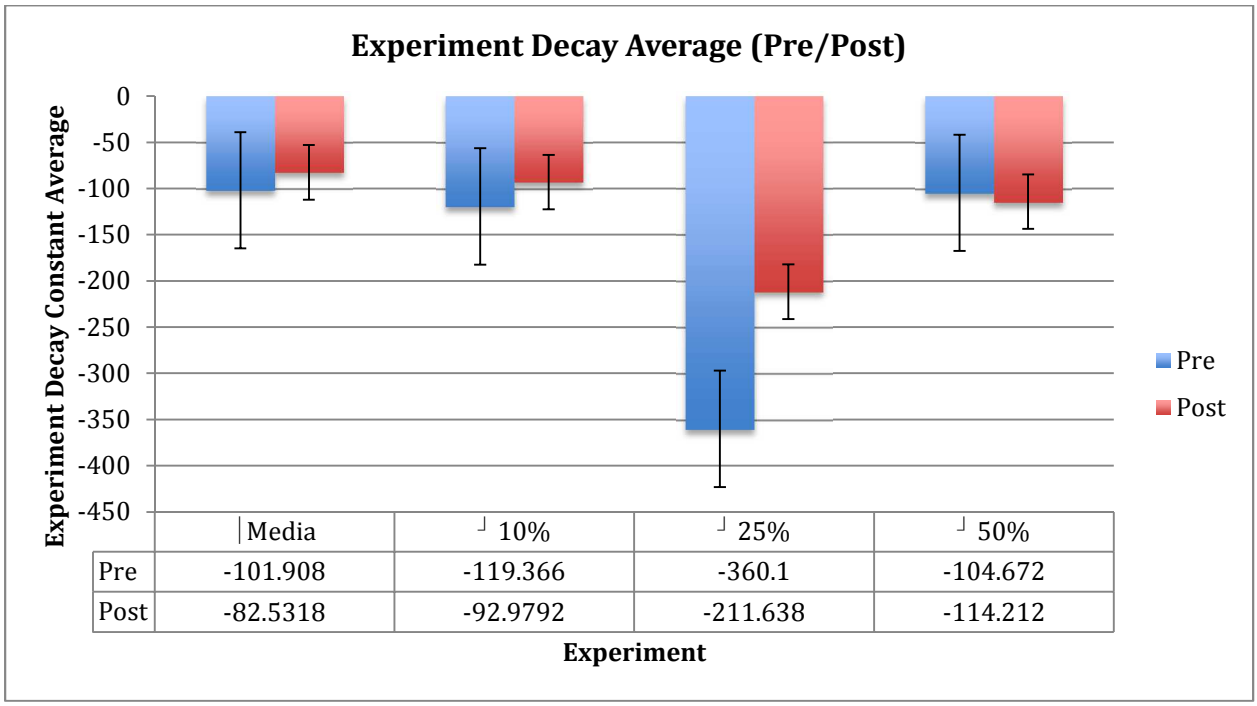

	Media	10%	25%	50%
Pre	-101.908	-119.366	-360.1	-104.672
Post	-82.5318	-92.9792	-211.638	-114.212

Figure 3.2 **Osmotic Experimental Decay Constant Averages for Pre-60s and Post-60s**.

The decay constants were taken from each trend line for each cell in each experiment shown in Table 3.2. The overall decay constants were majorly negative, with an occasion of a positive in pre-60s trend lines. This shows that over time there is decay in integrated density over time.

Table 3.2 **Osmotic Experimental Decay Constant Values of Each Cell.**

Cell Number	Experimental Group	Baseline Decay Constant (Linear-Pre)	Baseline Decay Constant (Linear-Post)	Experiment Decay Constant (Linear-Pre)	Experiment Decay Constant (Linear-Post)
1	Media	-40.53	-8.332	-46.38	-12.41
2	Media	-152.2	-63.52	-125.3	-104.7
3	Media	-152.2	-63.52	21.28	-45.54
4	Media	-51.79	3.498	-36.04	-9.709
5	Media	-340.6	72.47	-323.1	-240.3
1	Water 10%	72.49	-164.5	-63.01	-158.8
2	Water 10%	46.42	-101.4	-12.34	-72.8
3	Water 10%	-283	-154.6	-307.4	-114.7
4	Water 10%	-453	-347.1	-76.28	2.204
5	Water 10%	6.965	2.45	-137.8	-120.8
1	Water 25%	-24.81	-23.45	-16.1	-21.37
2	Water 25%	22.19	-281	-653	-411.6
3	Water 25%	119.5	-264.6	-377.2	-241.7
4	Water 25%	-58.16	-106.8	-581.4	-326.7
5	Water 25%	-197.5	-233.5	-172.8	-56.82
1	Water 50%	125.4	-17.29	-115.5	-84.41
2	Water 50%	-49.98	-77.17	-79.26	-113.4
3	Water 50%	-459	-213.8	-123.6	-82.77
4	Water 50%	-54.54	-2.612	13.2	-22.78
5	Water 50%	-207.2	-0.4737	-218.2	-267.7

3.2 TRPV-4 Inhibitor Testing

3.2.1 TRPV-4 Inhibitor Experimental Testing Results

Integrated Density was taken versus time to produce graphs for each experiment. These tests were done by using inhibitors HC-067047 and GSK-2193874 on DRG cells. Water and media were added post-inhibitor addition and integrated density versus time was taken. For HC-067047 experiments, baseline, water, and media resulted in decay over time. There is no jump between the minimum integrated densities of baseline and maximum integrated densities of post-addition of water or media for HC-067047 experiments (Figure S_{13}, S_{14}). For GSK-2193874, there is decay in both baseline and post-media addition (Figure S_{15}). In post-water addition for these experiments, there is decay for baseline results but addition of water produced a zero slope plot (Figure S_{16}). However, like HC-067047, in both there is no jump in intensity from minimum baseline intensity to the maximum intensity of both water and media.

Post/Pre ratio means were taken cumulatively of the 5 cells for each experiment and plotted on a bar graph with standard error of mean bars (Figure 3.3). All post/pre ratio means for both type of inhibitor result experiments resulted in a post/pre ratio mean of less than 1. Normalized integrated density was also plotted to account for area in these figures as well (Figure S_{13}, S_{14}, S_{15}, S_{16}).

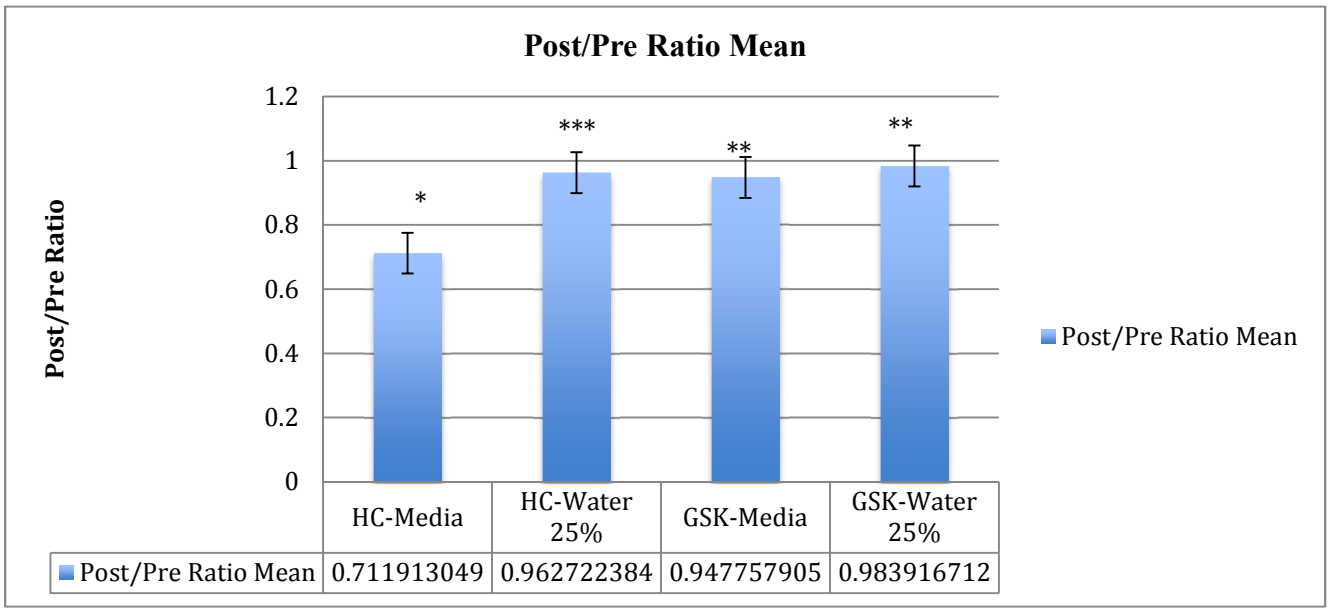

Figure 3.3 **TRPV-4 Inhibitor Post/Pre Ratio Means.** HC-067047-Media, HC-067047-Water 25%, GSK-2193874-Media, GSK-2193874-Water 25% resulted in a post/pre ratio mean of 0.711, 0.962, 0.947, and 0.984 respectively.
*Post-hoc comparison tests showed significant difference between HC-media tests vs. no inhibitor media tests and water tests.
***Post-hoc comparison tests showed significant difference between no inhibitor water tests and inhibitor water tests
**-Post-hoc comparison tests showed significant difference between no inhibitor water tests and both inhibitor water and media tests

The values of minimum intensity, maximum intensity, and the post/pre ratio of each cell in these experiments are shown in Table 3.3, representing what was shown in Figure 3.3.

Table 3.3 **TRPV-4 Inhibitor Results of Each Cell.**

Cell Number	Experimental Group	Minimum Intensity (Pre)	Maximum Intensity (Post)	Post/Pre Ratio
1	HC-067047 Media	23798	17270	0.725691235
2	HC-067047 Media	25932	15133	0.583564708
3	HC-067047 Media	13507	13435	0.994669431
4	HC-067047 Media	22343	14333	0.641498456
5	HC-067047 Media	24750	15200	0.614141414
1	HC-067047 Water	32053	25590	0.798365208
2	HC-067047 Water	41244	40031	0.970589662
3	HC-067047 Water	63451	54869	0.864746024
4	HC-067047 Water	64575	65481	1.014030197
5	HC-067047 Water	31601	36843	1.165880827
1	GSK-2193874 Media	36025	35482	0.984927134
2	GSK-2193874 Media	165620	142592	0.860958821
3	GSK-2193874 Media	71103	75002	1.054835942
4	GSK-2193874 Media	65014	60134	0.924939244
5	GSK-2193874 Media	145433	132799	0.913128382
1	GSK-2193874 Water	12439	9241.9	0.742977731
2	GSK-2193874 Water	13497	12508	0.926724457
3	GSK-2193874 Water	77907	72334	0.928465992
4	GSK-2193874 Water	33224	33574	1.010534553
5	GSK-2193874 Water	18721	24541	1.310880829

3.2.2 TRPV-4 Timed Inhibitor Experiment Results

Integrated Density was taken versus time to produce graphs for each experiment. This data was plotted at baseline (0 minutes), 20 minutes, and 45 minutes on the same graph. In all but 20 minute time points for both HC-067047 and GSK-2193874, there is decay over time as well as in comparison to in time imaged (Figure S_{21}). For HC-067047 and GSK-2193874, when imaged at 20 minutes there appeared to be a slight increase over time or a stagnant horizontal slope in integrated density. There were 5 cells imaged for each inhibitor experiment.

Post/Pre ratio means were taken cumulatively of the 5 cells for each experiment and plotted on a bar graph with standard error of mean bars (Figure 3.4). All post/pre ratio means for both type of inhibitor result experiments resulted in a post/pre ratio mean of less than 1. However, the post/pre ratio mean of 20 minutes to the baseline resulted in a higher post/pre ratio than the post/pre ratio mean of 45 minutes to the baseline. The values of minimum intensity, maximum intensity, and the post/pre ratio of each cell in these experiments are shown in Table 3.4, representing what was shown in Figure 3.4.

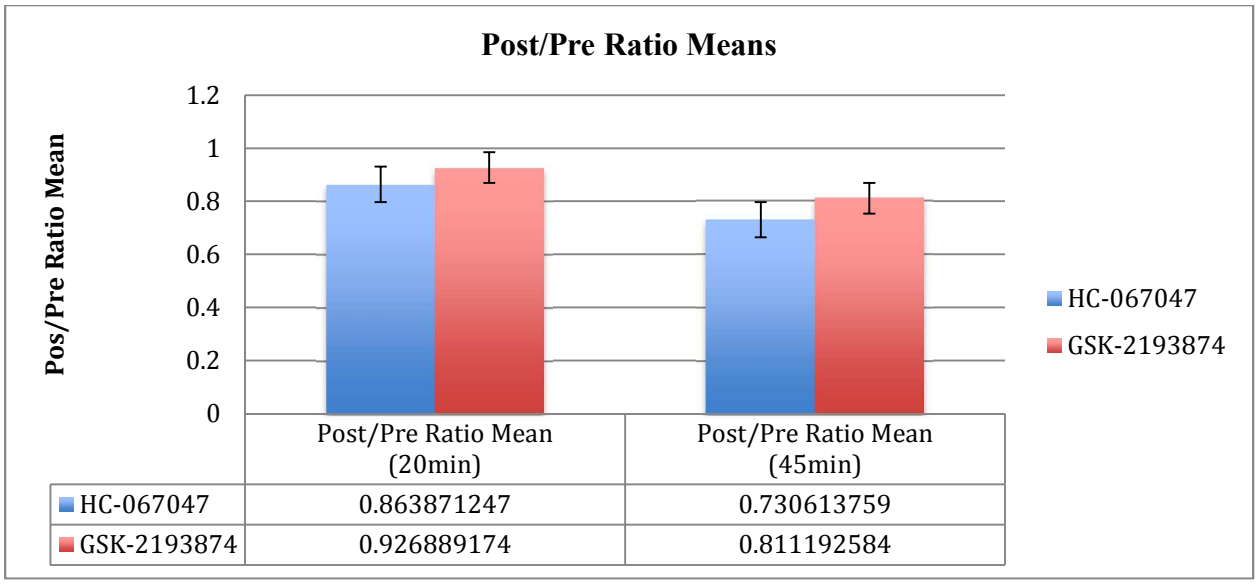

Figure 3.4 **TRPV-4 Inhibitor Timed Post/Pre Ratio Means.** HC-067047-20 minutes, HC-067047-45 minutes, GSK-2193874-20 minutes, and GSK-2193874-45 minutes resulted in 0.864, 0.731, 0.927, and 0.811 post/pre ratio means respectively.

Table 3.4 **TRPV-4 Inhibitor Timed Results for Each Cell.**

Cell Number	Experimental Group	Minimum Intensity (Pre-Baseline)	Maximum Intensity (Post-20 min)	Maximum Intensity (Post-45min)	Post/Pre Ratio (20min)	Post/Pre Ratio (45min)
1	HC-067047	111520	102084	88595	0.915387374	0.794431492
2	HC-067047	31450	30487	23606	0.969379968	0.750588235
3	HC-067047	31443	26988	22326	0.858315046	0.710046751
4	HC-067047	42745	35669	32176	0.834460171	0.752743011
5	HC-067047	33898	25146	21873	0.741813676	0.645259307
1	GSK-2193874	59968	58659	55140	0.978171692	0.919490395
2	GSK-2193874	106920	77001	46914	0.720173962	0.438776655
3	GSK-2193874	54291	56614	47996	1.042787939	0.884050763
4	GSK-2193874	63758	60183	58227	0.943928605	0.913250102
5	GSK-2193874	50379	47829	45361	0.949383672	0.900395006

3.2.3 TRPV-4 Inhibitor Trend Line Results

Trend lines for each graph were plotted to see the overall trend of each inhibitor experiment with media and water addition post inhibitor incubation. Following osmotic experiments, two linear fittings were deemed the best fit. The two linear fittings were used for the first 60 seconds, which seemed to be where the initial drop-off ended, and for that point onwards to 160 seconds exactly like those of osmotic pressure experiments (Figure S_{17}, S_{18}, S_{19}, S_{20}). For all cells in each experiment, there was an average decay in trend lines over the complete 3 minutes (Figure 3.5). These were the experiments done with media and water added post-inhibitor incubation. These values are listed in Table 3.5.

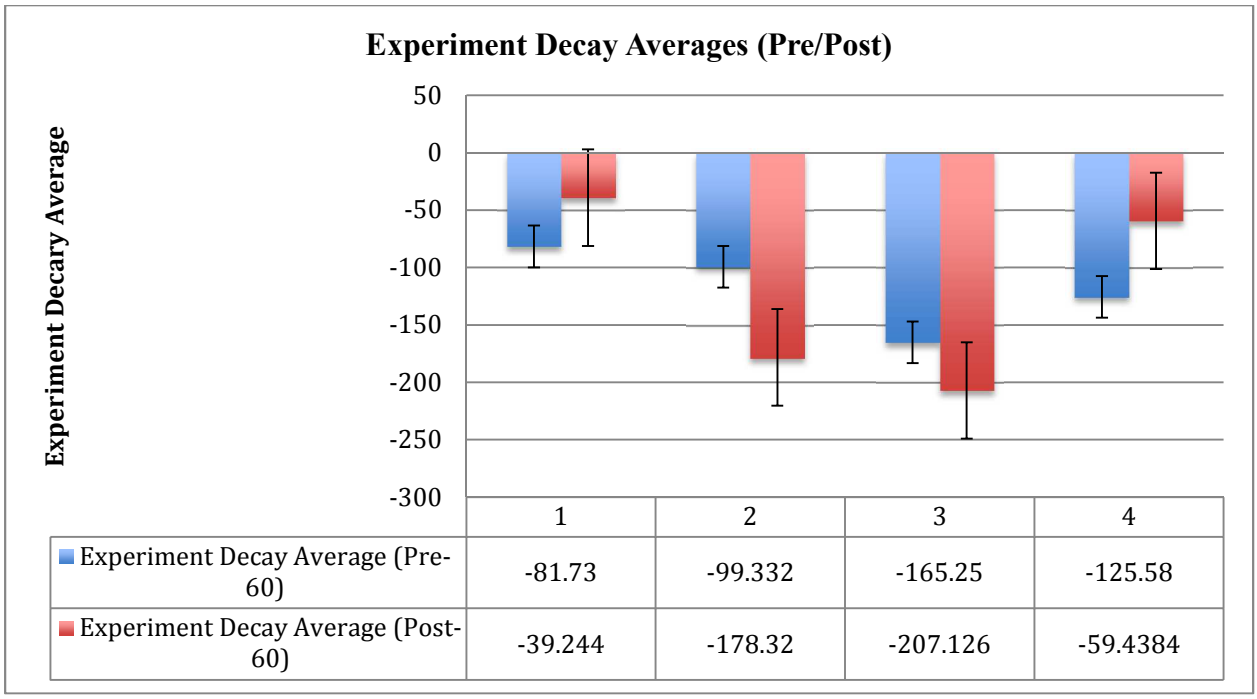

	1	2	3	4
Experiment Decay Average (Pre-60)	-81.73	-99.332	-165.25	-125.58
Experiment Decay Average (Post-60)	-39.244	-178.32	-207.126	-59.4384

Figure 3.5 **Inhibitor Experimental Decay Constant Averages for Pre-60s and Post-60s**.

The decay constants were taken from each trend line for each cell in each experiment shown in Table 3.5. The overall decay constants were majorly negative. This shows that over time there is decay in integrated density over time for all experiments.

Table 3.5 **Inhibitor Experimental Decay Constant Values.**

Cell Number	Experimental Group	Baseline Decay Constant (Linear-Pre)	Baseline Decay Constant (Linear-Post)	Experiment Decay Constant (Linear-Pre)	Experiment Decay Constant (Linear-Post)
1	HC-067047 Media	-72.96	-42.69	-113.2	-43.17
2	HC-067047 Media	-63.73	-47.91	-99.54	-41.16
3	HC-067047 Media	5.817	8.674	-49.91	-31.13
4	HC-067047 Media	-65.33	-45.39	-85.17	-45.65
5	HC-067047 Media	-71.33	-40.57	-60.83	-35.11
1	HC-067047 Water	-2.89	-8.87	-135.6	-59.8
2	HC-067047 Water	-122.1	-165.4	-122.4	-182.6
3	HC-067047 Water	-119.9	-202.1	-130.8	-233
4	HC-067047 Water	-99.08	-151.9	-56.45	-262
5	HC-067047 Water	-198.1	-79.36	-51.41	-154.2
1	GSK-2193874 Media	-101.4	-25.66	-14.82	-183.2
2	GSK-2193874 Media	-299.2	-62.06	-742.4	-770.4
3	GSK-2193874 Media	-33.08	-31.27	-33.59	-31.23
4	GSK-2193874 Media	-39.85	-28.71	-35.44	-30.13
5	GSK-2193874 Media	-237.48	-68.38	-54.33	-20.67
1	GSK-2193874 Water	-156.7	-82.3	-7.7	-2.422
2	GSK-2193874 Water	-131.2	-88.41	-3.781	-1.836
3	GSK-2193874 Water	-52.33	-46.8	-586.6	-274.7
4	GSK-2193874 Water	-188.4	-185.6	-7.359	-6.874
5	GSK-2193874 Water	-198.1	-102.4	-22.46	-11.36

3.3 Statistical Analysis

3.3.1 Osmotic Statistical Analysis

Statistical analysis was done on osmotic testing for post/pre ratios as well as both pre-60s and post-60s decay constants. This was done through a one-way ANOVA test. The p-value for post/pre ratio results had a p-value of 0.0132 demonstrating that there is significance in the effect of adding different levels of water. However, the p-value of pre-60s and post-60s decay constants exceeded the standard value of 0.05, which means that the varying input water levels did not have an effect on the system decay over time. These values are shown in Table 3.6. Post-hoc testing indicated a difference between 10% vs. 25% and 10% vs. 50% ($p<0.05$) shown in Figure 3.2. Though media ratios were lower than 25%/50% groups, these means were not significantly different.

Table 3.6 **Osmotic Experiment p-values.**

Osmotic Experiment	**p-value**
Osmotic Post/Pre Ratio	0.0132
Osmotic Pre-60 Decay Constants	0.0684
Osmotic Post-60s Decay Constants	0.28123

3.3.2 TRPV-4 Inhibitor Statistical Analysis

Statistical Analysis was done on inhibitor testing for post/pre ratios as well as both pre-60 and post-60s decay constants. This was done through a two-way ANOVA test. The p-value for HC-067047 experiments resulted in a value of 0.00041 for Factor 1 (Inhibitor/No Inhibitor). This meant that there was significance in the effect of adding an inhibitor compared to not having an inhibitor. The value for Factor 2 (Water/Media) was 0.00782. This meant that there was significance in the effect of adding water or media to the system. However, the conjunctive p-value between the factors was 0.84657 showing that there is no significance in the interaction between Factor 1 and 2 (Table 3.7). For HC-067047, post-hoc testing indicated a difference between media with the inhibitor and 25% water with no inhibitor as well as for 25% water and media tests with and without the inhibitor ($p<0.05$) shown in Figure 3.3.

Table 3.7 **HC-067047 Inhibitor Experiments Post/Pre Ratio p-value.**

HC-067047 Inhibitor Experiments	**p-value**
Factor #1 (Inhibitor/No Inhibitor)	0.00041
Factor #2 (Water/Media)	0.00782
Factor #1 + #2	0.84657

Another two-way ANOVA test was done for the decay constants to get the p-values. The p-values for all factors was greater than 0.05. This shows no significance in effect of the factors on the decay of

integrated density over time (Table 3.8). However, post-hoc comparison showed that there was a significant difference between 25% water tests between having whether or not an inhibitor was involved.

Table 3.8 **HC-067047 Inhibitor Experiments Pre-60s and Post-60s Decay Constant p-value**

HC-067047 Inhibitor Experiments	**Pre-60s Decay Constant p-value**	**Post-60s Decay Constant p-value**
Factor #1 (Inhibitor/No Inhibitor)	0.05555	0.4262
Factor #2 (Water/Media)	0.09609	0.91669
Factor #1 + #2	0.05967	0.01138

The p-value for GSK-2193874 experiments resulted in a value of 0.00886 for Factor 1 (Inhibitor/No Inhibitor). This meant that there was significance in the effect of adding an inhibitor compared to not having an inhibitor. The value for Factor 2 (Water/Media) was 0.08767. This meant that there was no significance in the effect of adding water or media to the system. However, the conjunctive p-value between the factors was 0.17766 showing that there is no significance in the interaction between Factor 1 and 2 (Table 3.9). For GSK-2193874, post-hoc testing indicated a difference between water testing without an inhibitor versus inhibitor testing for both media and 25% water ($p<0.05$) shown in Figure 3.3.

Table 3.9 **GSK-2193874 Inhibitor Experiments Post/Pre Ratio p-value**

GSK-2193874 Inhibitor Experiments	**p-value**
Factor #1 (Inhibitor/No Inhibitor)	0.00886
Factor #2 (Water/Media)	0.08767
Factor #1 + #2	0.17766

Another two-way ANOVA test was done for the decay constants to get the p-values. The p-values for all factors was greater than 0.05. This shows no significance in effect of the factors on the decay of integrated density over time (Table 3.10).

Table 3.10 **GSK-2193874 Inhibitor Experiments Pre-60s and Post-60s Decay Constant p-value**

GSK-2193874 Inhibitor Experiments	**Pre-60s Decay Constant p-value**	**Post-60s Decay Constant p-value**
Factor #1 (Inhibitor/No Inhibitor)	0.48968	0.87778
Factor #2 (Water/Media)	0.37331	0.91754
Factor #1 + #2	0.19216	0.13671

3.3.3 TRPV-4 Timed Inhibitor Statistical Analysis

A one-way ANOVA test was done on both inhibitors separately to get the p-value with a factor based on time. The p-value for HC-067047 was 0.01991 and is less than 0.05, which meant that there is an effect on the system through time. The p-value for GSK-2193847 had a p-value of 0.3157, which is more than 0.05, which meant that there is no significance in time on this specific inhibitor experiment (Table 3.11).

Table 3.11 **Timed Inhibitor Experiments p-value**

Timed Inhibitor Experiments	**p-value**
HC-067047 Timed Inhibitor Experiments	0.0199
GSK-2193874 Timed Inhibitor Experiments	0.0697

Chapter 4: Discussion

4.1 Osmotic Testing

The primary purpose of osmotic testing in this study was to determine the mechanical effect of adding water and media. Adding media provided a constant variable to the experiment in order to see if there were any specific mechanical changes compared to adding water, which theoretically would activate

calcium channels. Media experiments resulted in the same calcium levels at the end of baseline measurements to the adding of media. This shows that media did not activate calcium channels, which was expected. The decay in these experiments over time could be accounted for by photo bleaching. Adding water was the variable change in the experiment to compare the changes in integrated density, which accounts for the activation of calcium channels. There was an overall decay in all experiments performed in this study. This is most likely accounted for through photo bleaching over time while performing calcium imaging. Specifically in baseline testing for all experiments, photo bleaching account so for the majority of the decay. In osmotic testing, excluding 10% water addition, there is a rapid influx of calcium represented by the increase in integrated density from the addition of 25% and 50% water. This is primarily due to osmotic swelling due to tonicity properties and water diffusion. The addition of water causes water to rush into the cell thereby activating calcium channels to restore proper levels of calcium. This leads to the jump in integrated density levels from baseline to addition of water shown in Figure S_3 and S_4. After calcium increase due to water swelling, over time there is a restoration of calcium levels and a reduction of swelling leading to a decrease of calcium levels over time. Reduction in calcium levels in 25% and 50% water experimentation is also affected by photo bleaching slightly. 10% water addition had no increased levels of calcium, which can be assumed that the lower levels of water was not enough to activate osmotic swelling properties. This is shown through the post/pre ratio means of these osmotic experiments where the value increases over 1 considerably with each increase of water concentration. For this study, 25% water was decided to be used later on in inhibitor experiments, as this seemed to be a good standard of increased post/pre ratio values in this part of the study. The overall decay in this experiment can be accounted for by photo bleaching. Photo bleaching seemed to primarily slow down over time as well shown through two linear fits where the majority of experiments resulted in a more positive slope in the secondary linear fit as compared to the primary linear fit.

Statistical analysis showed promising results in osmotic testing. While the effect of water level input on decay constant did not show significance probably due to some limitations that will be covered on later in this study, there is an effect of water level input on the post/pre ratio. This meant that with the

increase of water there is more activation of calcium channels. This statistical analysis provides concrete evidence through ANOVA testing that water does have an effect on the system, and provides a starting point in future studies, such as the TRPV-4 inhibitor study. The trend shows a difference between adding water above 25%, but did not show statistical significant difference between media (0% water) and 25%/50% groups. This could be caused by the limitation of sample size in this study.

4.2 TRPV-4 Inhibitor Testing

4.1.1 TRPV-4 Inhibitor Testing

The primary purpose of these TRPV-4 inhibitor-testing experiments was to see if there is an effect of these inhibitors on DRG calcium channels. The plates were incubated with the inhibitors for 45 minutes in order to allow time for the cells to absorb the inhibitor. Studies have shown that these inhibitors proved effective after around 45 minutes to 2 hours of incubation, which is why these plates were incubated for 45 minutes. Adding media was set as a constant variable in order to compare the effect of adding water after inhibitor absorption. Through osmotic experiments, it was seen that adding water activates the calcium channels through osmotic swelling, allowing more calcium to influx. Conversely, adding media in these experiments did not change the integrated density of calcium, and the maximum integrated density of media was maintained at the minimum level of baseline. However, seen by the results in inhibitor testing, adding water post inhibitor incubation demonstrated similar results to adding media. For both solution additions, the results mimicked the results in osmotic testing for media. The minimum integrated density of the baselines remained higher than the maximum integrated density after the addition of media or water. This is further analytically shown through the average post/pre mean ratios after water addition in which these values remain less than 1 and close to the values of media, which remains as a control. This illustrates that TRPV-4 channel inhibitors have some sort of effect in blocking calcium influx to the system and preventing osmotic swelling dynamics. In all experiments for this testing, the overall decay should primarily be in due part by photo bleaching. Photo bleaching seemed

to primarily slow down over time as well shown through two linear fits where the majority of experiments resulted in a more positive slope in the secondary linear fit as compared to the primary linear fit.

Statistical analysis for HC-067047 showed promising results, as for both the factors of if there is an inhibitor or no inhibitor and if there is an addition of water or a control media, the p-value was less than 0.05. This showed that there was significance on the effect of having an inhibitor or not. This supported that the post/pre ratio resulting in values of less than 1. In addition, adding water or media had an effect on the system as well, which is a little strange, as theoretically the inhibitor should be blocking the effect calcium channels. However, this could possibly be misconstrued as this includes data of both osmotic control data and inhibitor data to be compared in the ANOVA two-way test. The last part of this ANOVA test checked to see if there is an interaction between factor 1 and factor 2, which proved to be not significant as there was a p-value greater than 0.05. This meant that there was no effect between the interaction between factor 1 and factor 2 unfortunately. However, this could be possibly accounted for due to the limitations in the study to be discussed further in the study. There was no shown significance on decay constants based on the inhibitors or addition of water or media. Through post-hoc comparison testing, there was no significance difference between media and no inhibitor compared to 25% with an inhibitor. This meant that water experiments with the inhibitor showed similar results to the control of having no inhibitor tested with media. This meant that the results were significant. In addition post-hoc testing showed that there was significance between media testing between with or without an inhibitor, meaning that the inhibitor worked to some degree to further limit interactions with the control as well. There was also significance between water testing with or without an inhibitor, which meant that the inhibitor was working to limit calcium influx in the system. Lastly, there was huge significant difference between media with the inhibitor testing and water testing without the inhibitor. This proves the hypothesis, as the control was significantly different when compared to adding water, which should add calcium influx.

Statistical analysis for GSK-2193874 showed similar results to HC-067047. These results showed that there was an effect that occurs when there is an inhibitor or not, as the p-value for this test was less

than 0.05. However, for factor 2 in adding water and media, there showed to be no significance although the value was only slightly greater than 0.05. This could possibly be accounted for by the number of cells done in this study, which is a limitation to be further discussed. Similar to HC-067047, there was no effect between the interaction between factor 1 and 2. This could also be due to the numerous amounts of limitations throughout this study. Through post-hoc comparison testing, there was no significance difference between media and no inhibitor compared to 25% with an inhibitor. This meant that water experiments with the inhibitor showed similar results to the control of having no inhibitor tested with media. This meant that the results were significant. In addition post-hoc testing showed that there was significance between media testing between with or without an inhibitor, meaning that the inhibitor worked to some degree to further limit interactions with the control as well. There was also significance between water testing with or without an inhibitor, which meant that the inhibitor was working to limit calcium influx in the system. Lastly, there was huge significant difference between media with the inhibitor testing and water testing without the inhibitor. This proves the hypothesis, as the control was significantly different when compared to adding water, which should add calcium influx. GSK-2193874 had similar results with HC-067047 in post-hoc comparison. There was also no significance difference between media and no inhibitor compared to 25% with an inhibitor. This shows that despite adding water to the system, there is no change in calcium activity compared to the control. In addition, inhibitor experiments on both media and water showed significant difference to 25% water testing with no inhibitor. This means that the inhibitor itself is working, and it is limiting calcium influx to an extent.

4.1.2 TRPV-4 Timed Inhibitor Testing

In order to test the timeframe of the effect of the inhibitor, data from cells was taken during the course of incubation with the inhibitor in order to see its effect over the course of time. Time points were taken at baseline (0 minutes), 20 minutes, and 45 minutes. As studies have shown that these inhibitors proved effective from time points 45 minutes to 2 hours of incubation, 45 minutes was chosen as the point for the aforementioned inhibitor testing, as well as the end point for the TRPV-4 timed inhibitor testing. 20 minutes was chosen as a middle point of absorption to see if the inhibitors had some sort of effect

when not in the effective time zone. Results showed that at 20 minutes there remains a stagnant horizontal slope after baseline measurements. In contrast, at 45 minutes it remains to be decay over time. Specifically, the post-pre mean ratio of these showed to be less for 45 minutes than it was for 20 minutes. This meant that over time, the maximum integrated density measured at 45 minutes resulted in a less value than at 20 minutes. This illustrates that there is, but limited, an effect of absorption of inhibitors on the effect of calcium absorption. However, as this study is limited there is no account for photo bleaching taking a part of the increased decay over time.

Statistical analysis for timed inhibitor experiments showed different results between HC-067047 and GSK-2193874. For HC-067047, the p-value was less than 0.05 and showed significance. This meant that time had some sort of effect on the overall system. For GSK-2193874, the p-value was greater than 0.05 and showed no significance. These results seemed a little bit off, as for both inhibitors, the trend graphs of integrated density showed similar trends. However, more concrete significance can maybe be done through adding more cell subjects to the study and increasing the sample size.

4.3 Limitations

As this study focuses on a small part of a bigger picture on the inter-cellular dynamics of DRGs, there are many limitations to this study. In osmotic experiments, the results came with fruition, as the expected results were proven true by the experiments. In this case, one of the main limitations is the sample size of the experiments. While statistical analysis showed these experiments to be significant, it is important to have a big sample size to solidify the results as consistent. One other major limitation that occurs during these experiments is photo bleaching. Not only does this apply to this portion of osmotic experiments, but throughout the whole study. In order to account for this, there are some programs that would be able to identify and correct the data based on photo bleaching rate obtained through separate experimentation by testing the fluctuation of reduced light exposure and such. In some cases, this photo bleaching value could possibly be obtained through the system used depending on the complexity of the machine. An alternative to this, which was also implemented in this study, is to reduce the time-span of

light exposure thereby reducing the frequency and photon energy of input light that causes photo bleaching. This method could also be timed in order to check the variation of time affecting photo bleaching. Another is to research and implement more robust forms of fluorophores that are less prone to bleaching.

In TRPV-4 inhibitor experiments, the same limitations occur similar to osmotic experiments; however, there are more limitations in addition to those. One limitation is to test more specific inhibitors as well, to get an overall sense of the effect of each specific inhibitor. Like osmotic experiments, one important factor that needs to be re-iterated is the amount of sample size, as different than osmotic experiments, there is more variation in statistical analysis with some having a value close to 0.05 but only slightly higher. Increasing the sample size, would allow for more concrete results whether or not the factors have an actual effect on the experiments.

In TRPV-4 timed inhibitor experiments, the same limitations occur as prior in this study. However, one important test is to repeat the same experiments with media added instead of inhibitors to serve as more of a control to the experiments. This would allow seeing the difference in result trends more clearly. In addition, to take it one step further, water could be added as a variable at the time points to see if there is an effect on the cells at different time points. In addition, there are different types of calcium channels such as other mechano-sensitive channels that could also have a different side effect that are not affected by TRPV-4 inhibition. These need to be accounted for in order to fully know the extent of inhibitor effect on calcium levels in DRGs.

In an overall methods sense for the preparation of these experiments, one other limitation is the health of the different cells taken and harvests done. Finding a way to qualitatively, and possible quantitatively grow cells healthily equally could be an important factor on the results. In addition, common practice methods could also have had an impact on the results, such as sterilizing properly to prevent contamination or misuse of pipetting. All these miniscule types of limitations that may have been overlooked could have an overall effect on the results that cannot be foreseen. This can be minimized by

mentally making sure common practices are held to the highest extent as well as by doing more experiments to create a bigger sample size.

4.4 Future Works

As mentioned in the background and literature review of this study, paclitaxel is a popular chemotherapeutic that has certain neuropathy effects. In order to improve cancer outcomes, it is a priority in order to predict and reduce paclitaxel-related neuropathy. There have been several studies that suggest that paclitaxel influences the effect of TRPV-4 channels. In addition, in the overall picture, paclitaxel affects the normal structure and mechanics of microtubules causing a rigid cytoskeleton. Theoretically, by reducing tau this could restore normal structure and function. Further tests from this study could be built off of this. So far in this study, only wild type mice have been used to test the fluctuation of calcium levels based on osmotic pressures and TRPV-4 inhibitors. By introducing using tau knockout mice and cells incubated in paclitaxel, this can send a bigger picture on the effect on calcium levels when introduced to this new system. This would be a more focused study that could illustrate the maximum efficiency of TRPV-4 inhibitors on these types of variables. In contrast, agonists can also be used instead of inhibitors to see the effect on these types of variables. Previous literature has suggested that TRPV-4 modulates paclitaxel-induced excitability or increased calcium influx. Whether to reduce excitability or increase calcium influx and its effect on neuropathy in paclitaxel influenced cells remains to be seen. However, researching the effects of these and which would help reduce peripheral neuropathy in paclitaxel treatment would prove to be a major key to help advance the treatments for cancer. While there are still many factors to take into consideration in such a broad field, research in this aspect of focus would provide a starting ground for research in the treatments for cancer.

Author contributions statement

Author contributions: A.C. and S.S. designed research; A.C. analyzed the data and performed statistical measurements; A.C. wrote the paper with input of principal investigator, S.S.

Supplemental Information

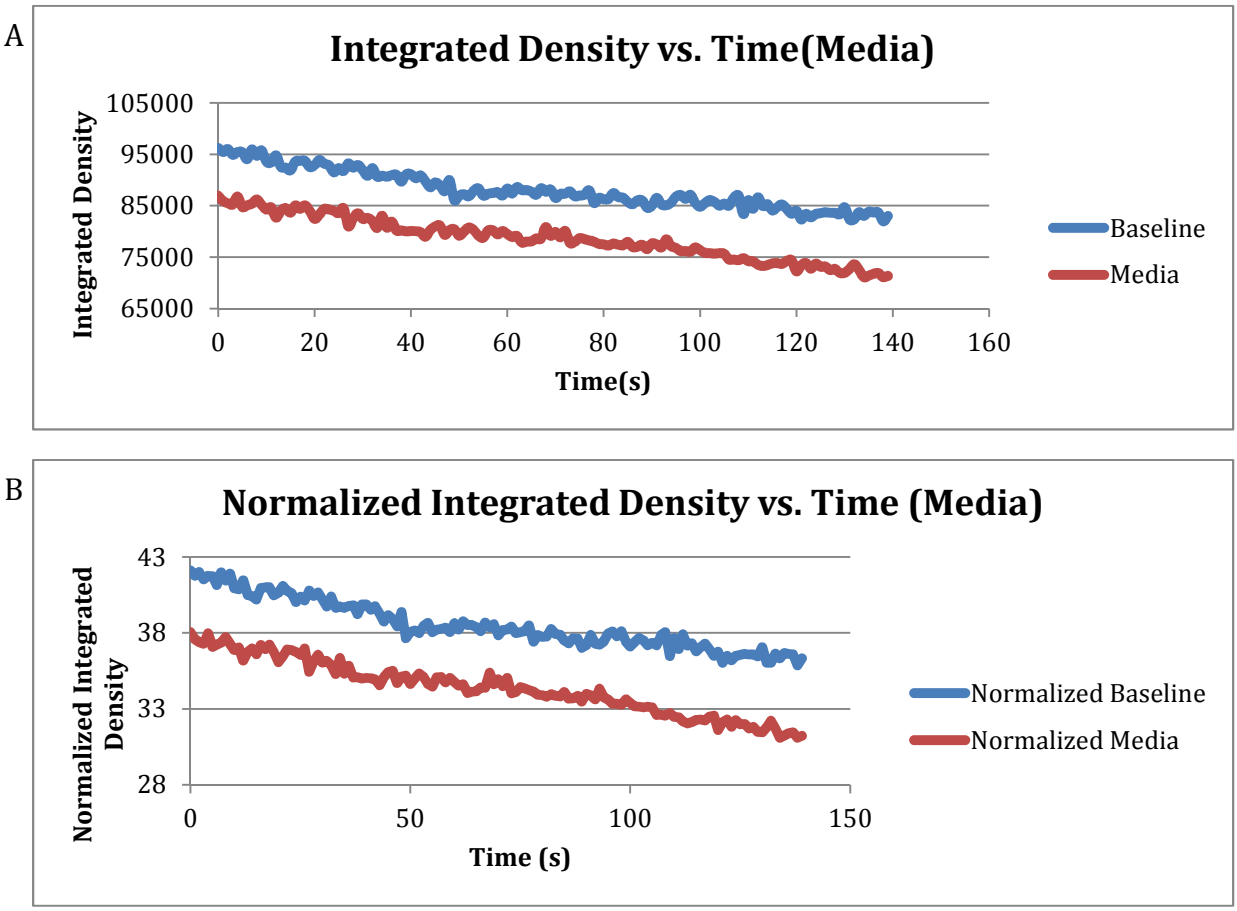

Figure S_1 **Media experiment graphs. A.** Integrated density vs. time combined graph of baseline testing and with media addition. **B.** Normalized integrated density vs. time combined graph of baseline testing and with media addition. Normalized integrated density was taken by dividing the density value by cell area.

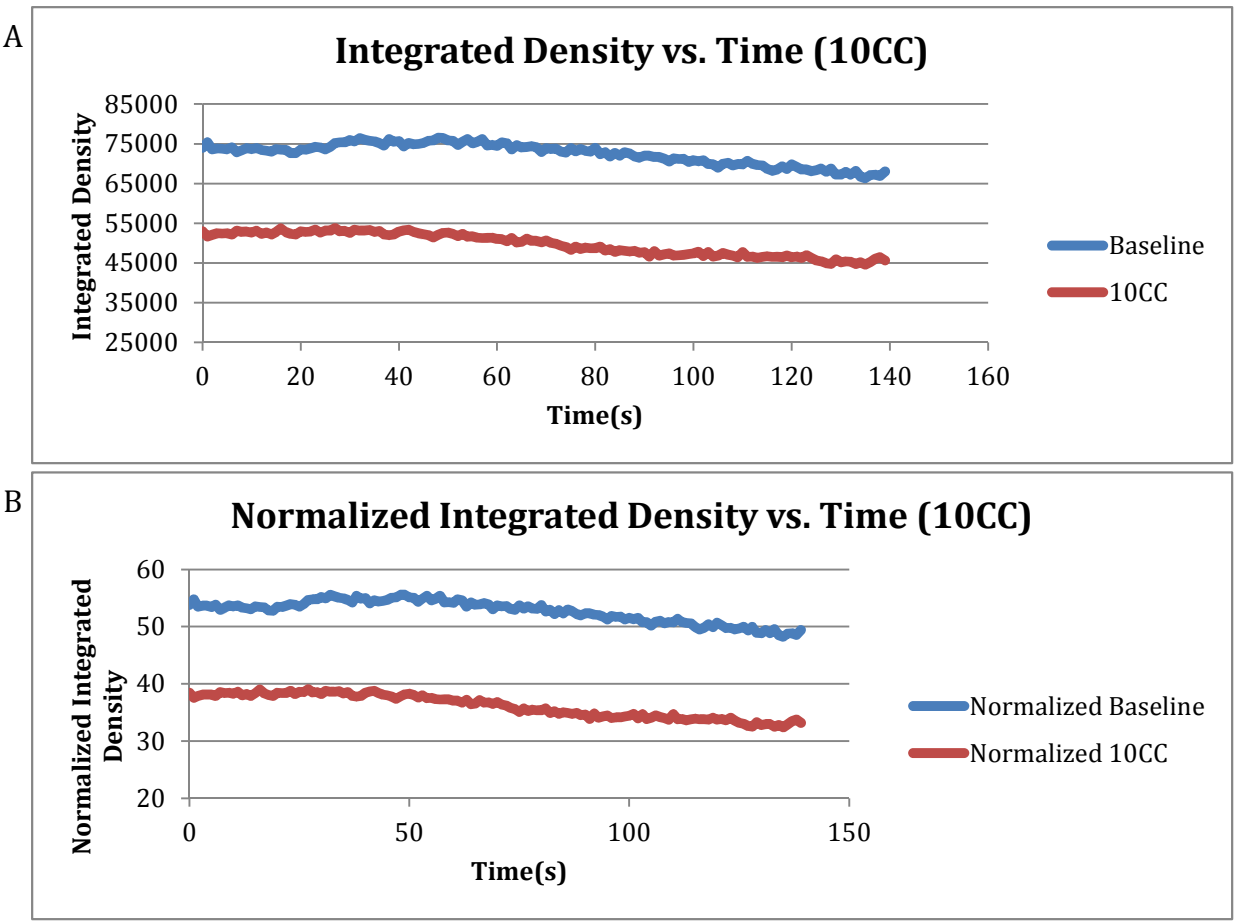

Figure S_2 **10% osmotic testing graphs.** A. Integrated density vs. time combined graph of baseline testing and with 10% water addition. B. Normalized integrated density vs. time combined graph of baseline testing and with 10% water addition. Normalized integrated density was taken by dividing the density value by cell area.

A

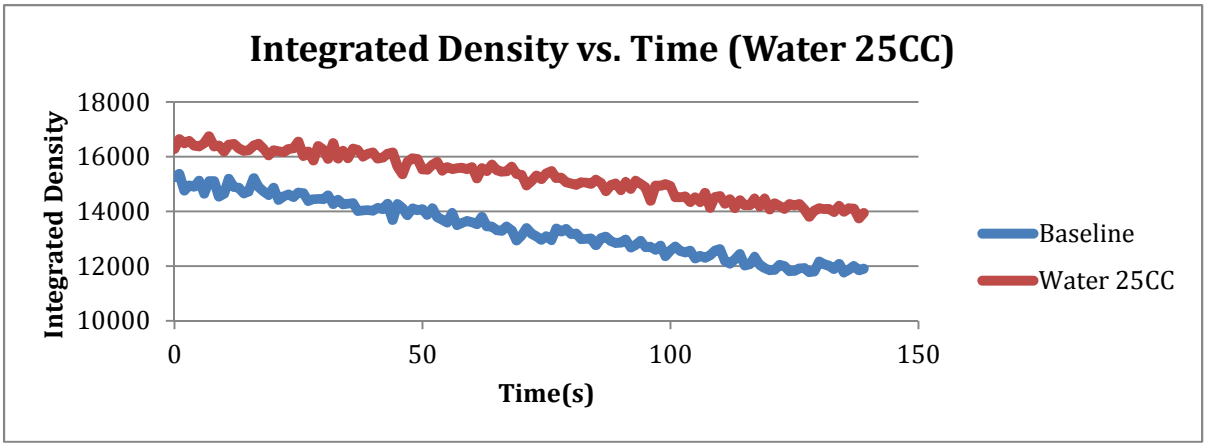

B

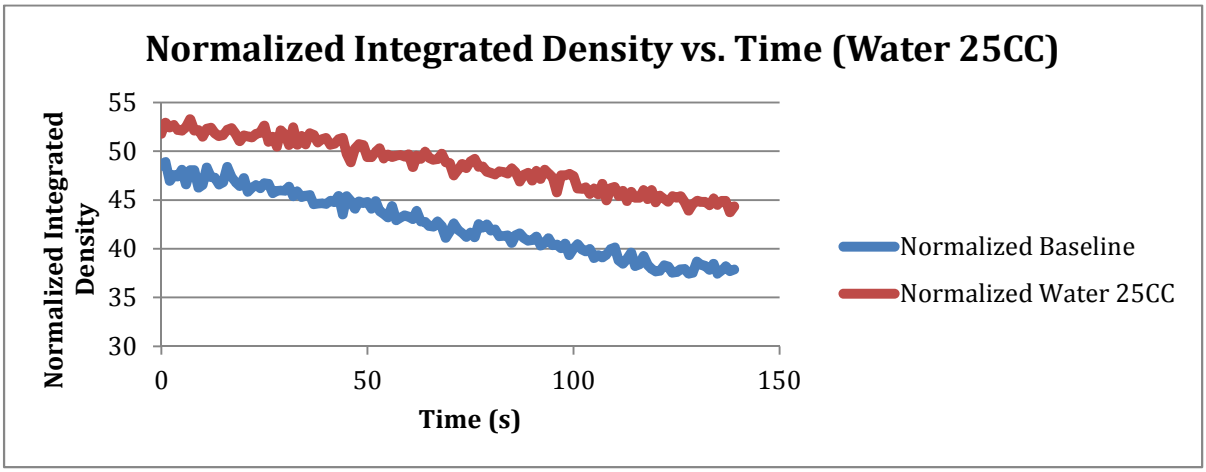

Figure S_3 **25% osmotic testing graphs.** A. Integrated density vs. time combined graph of baseline testing and with 25% water addition. B. Normalized integrated density vs. time combined graph of baseline testing and with 25% water addition. Normalized integrated density was taken by dividing the density value by cell area.

A

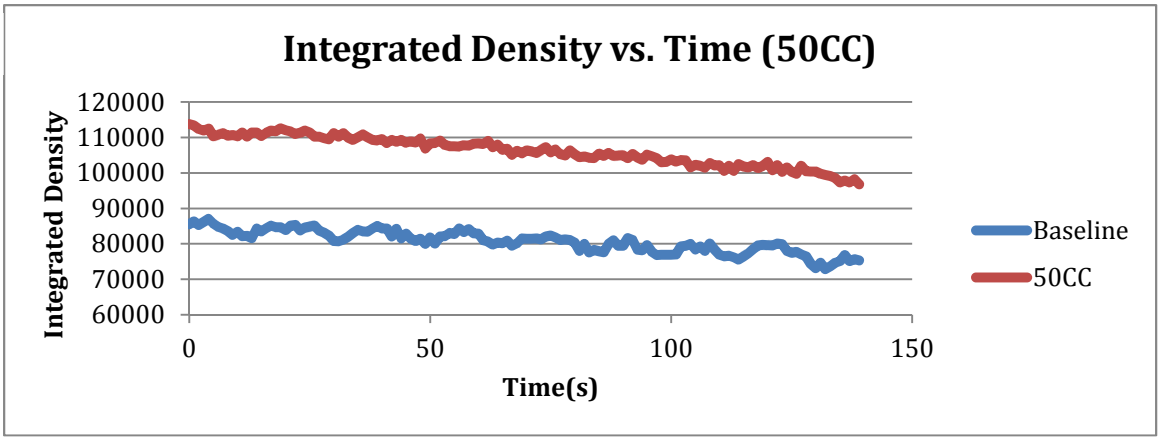

B

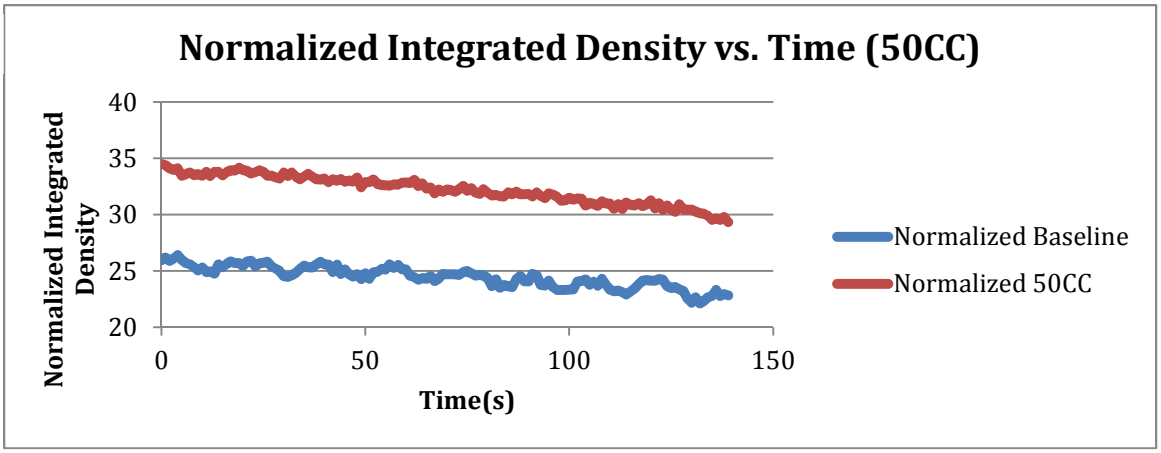

Figure S4 **50% osmotic testing graphs. A.** Integrated density vs. time combined graph of baseline testing and with 50% water addition. **B.** Normalized integrated density vs. time combined graph of baseline testing and with 50% water addition. Normalized integrated density was taken by dividing the density value by cell area.

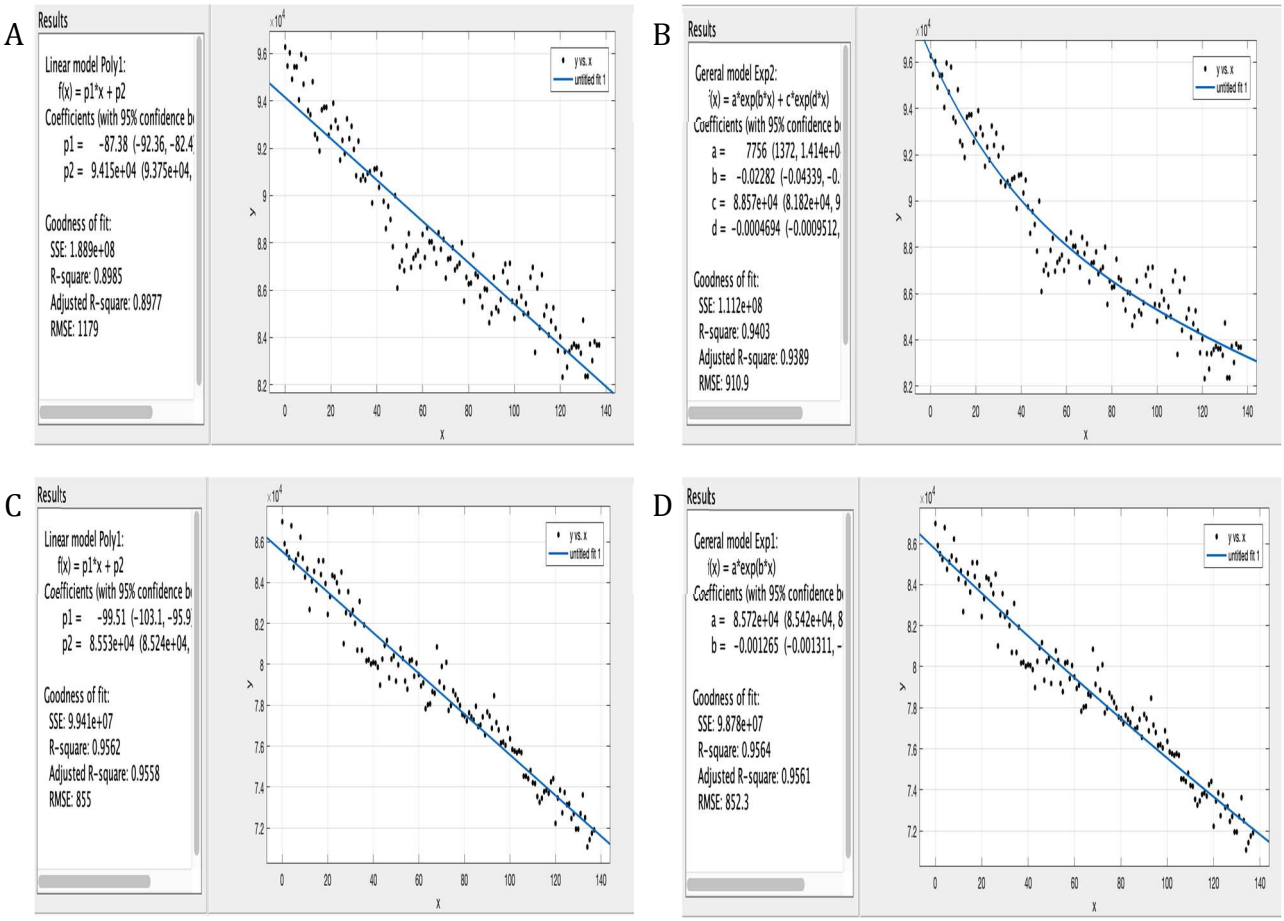

Figure S_5 **Media experiment trend-line graph. A.** Baseline linear graph of integrated density vs. time. **B.** Baseline exponential graph of integrated density vs. time. **C.** Post-media addition linear graph of integrated density vs. time. **D.** Post-media addition exponential graph of integrated density vs. time.

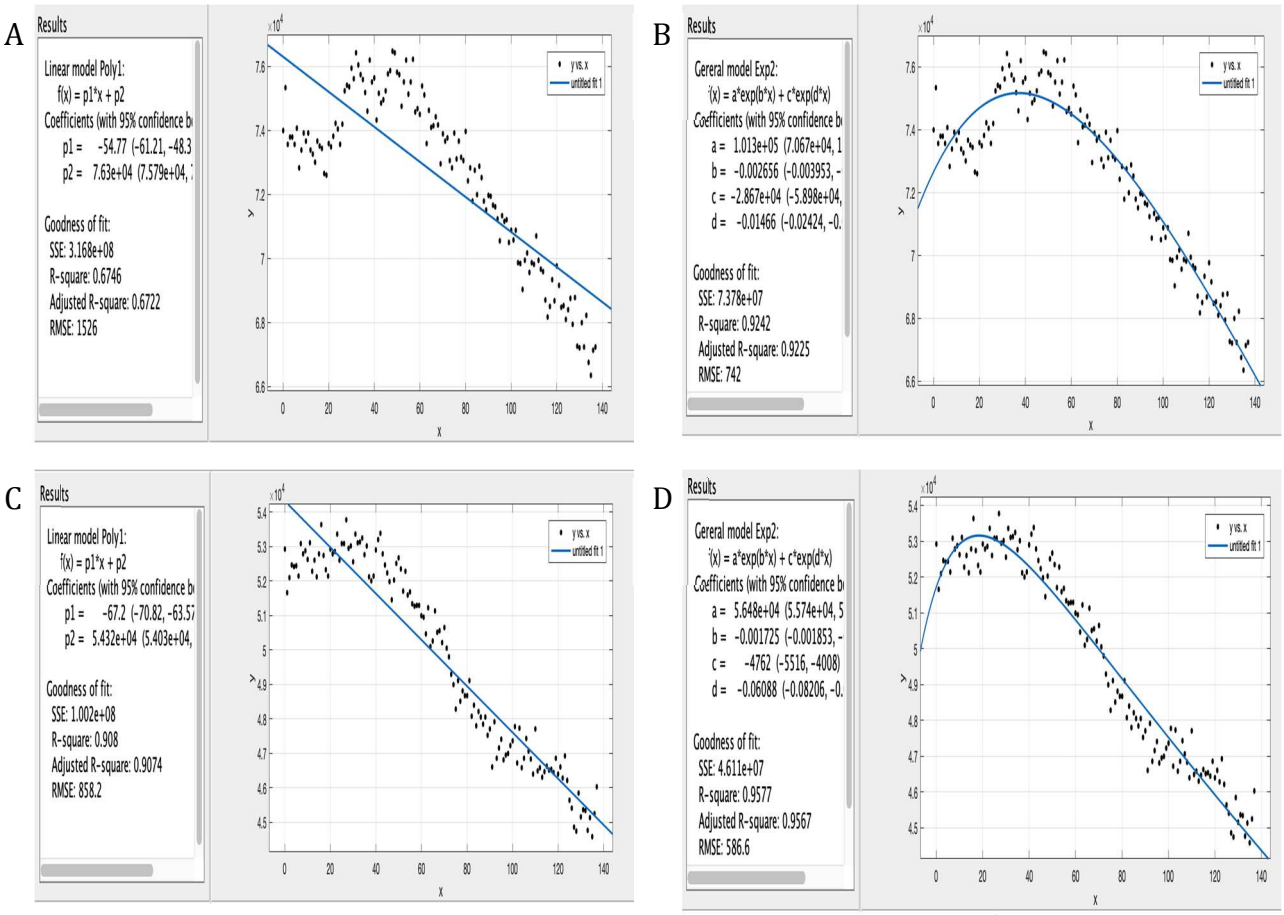

Figure S_6 **10% water testing trend-line graph. A.** Baseline linear graph of integrated density vs. time. **B.** Baseline exponential graph of integrated density vs. time. **C.** Post-water addition linear graph of integrated density vs. time. **D.** Post-water addition exponential graph of integrated density vs. time.

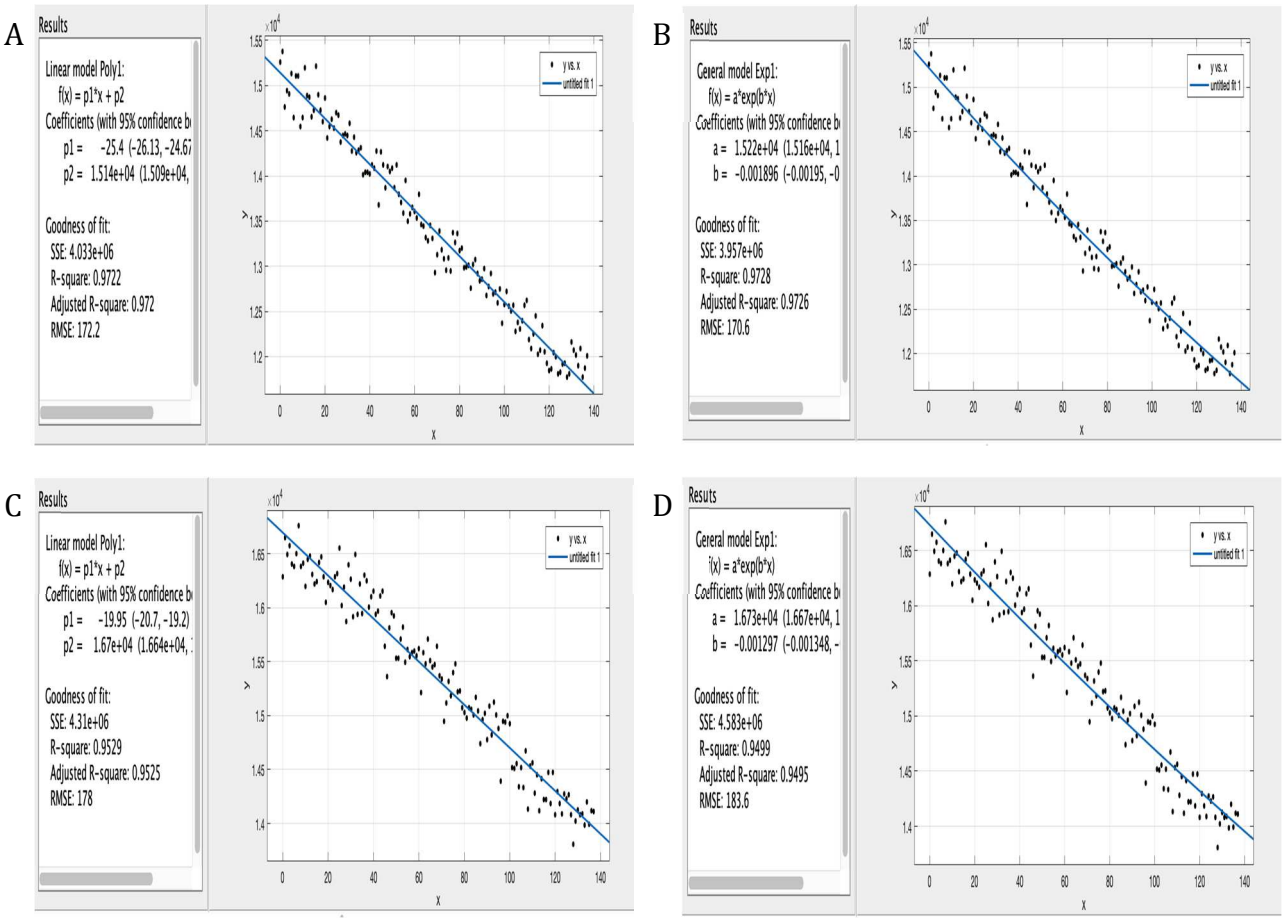

Figure S_7 **25% water testing trend-line graph. A.** Baseline linear graph of integrated density vs. time. **B.** Baseline exponential graph of integrated density vs. time. **C.** Post-water addition linear graph of integrated density vs. time. **D.** Post-water addition exponential graph of integrated density vs. time.

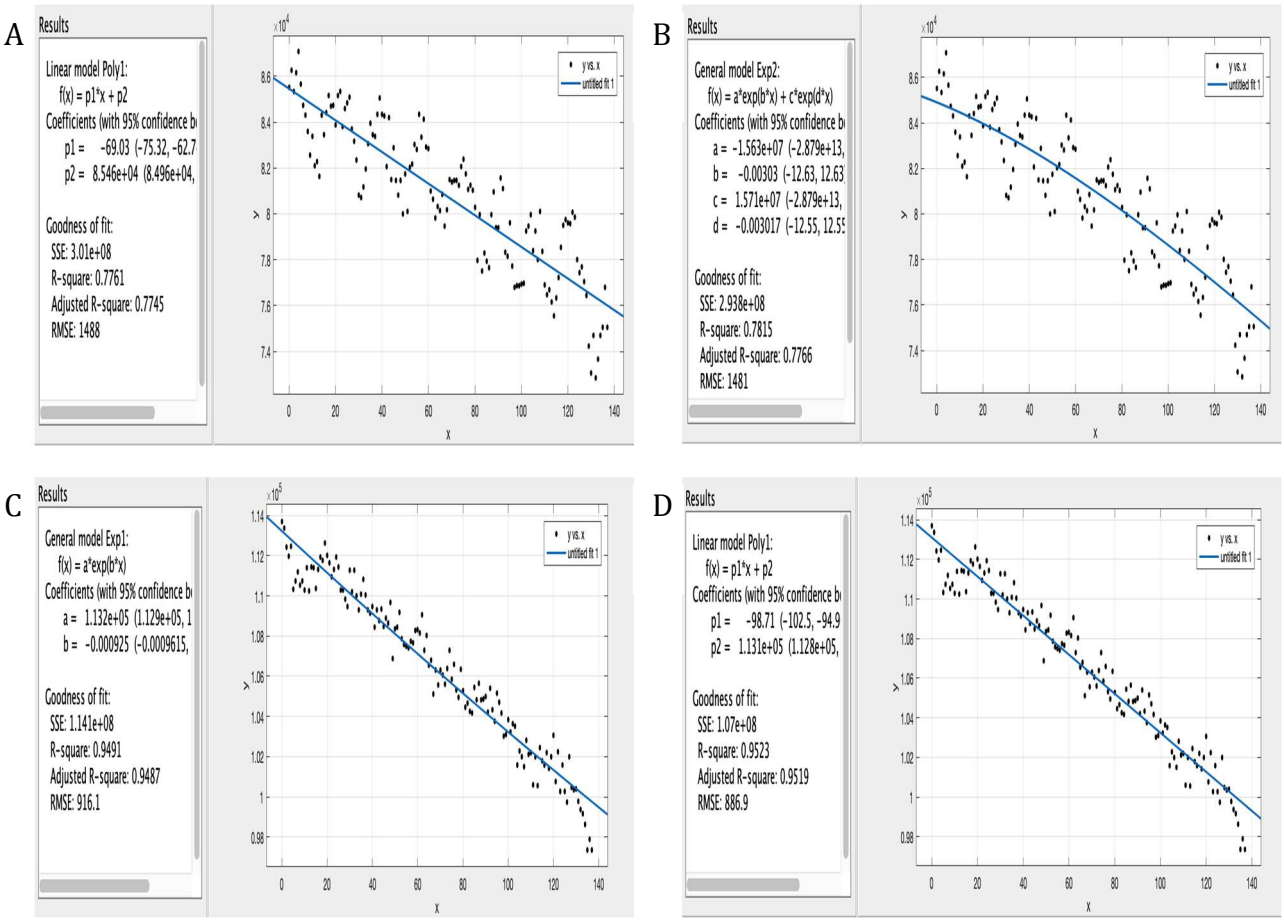

Figure S_8 **50% water testing trend-line graph. A.** Baseline linear graph of integrated density vs. time. **B.** Baseline exponential graph of integrated density vs. time. **C.** Post-water addition linear graph of integrated density vs. time. **D.** Post-water addition exponential graph of integrated density vs. time.

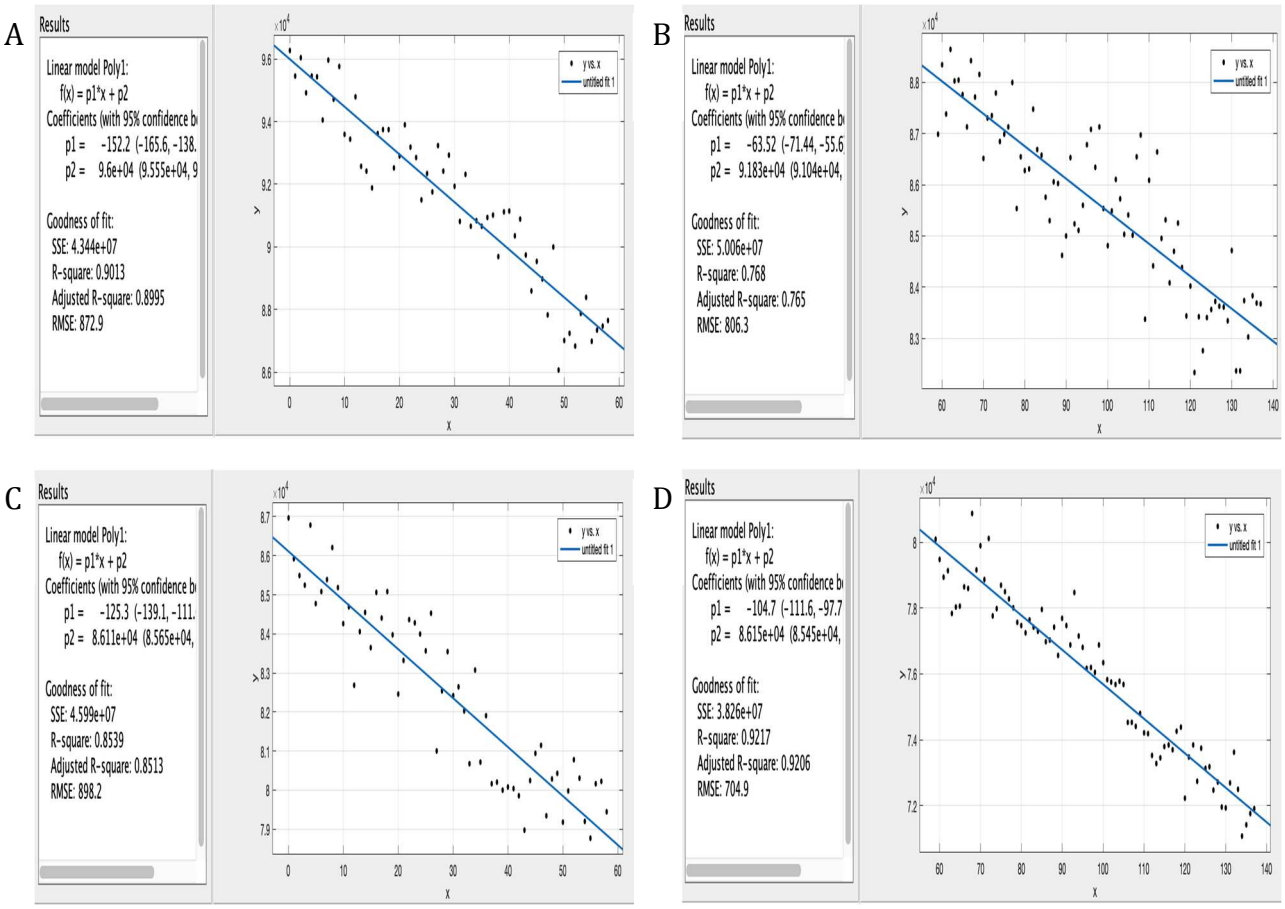

Figure S_9 **Media testing split trend-line graph at time point 60 seconds. A.** Baseline linear graph of integrated density vs. time (Pre-60s). **B.** Baseline linear graph of integrated density vs. time (Post-60s). **C.** Post-media addition linear graph of integrated density vs. time (Pre-60s). **D.** Post-media addition linear graph of integrated density vs. time (Post-60s).

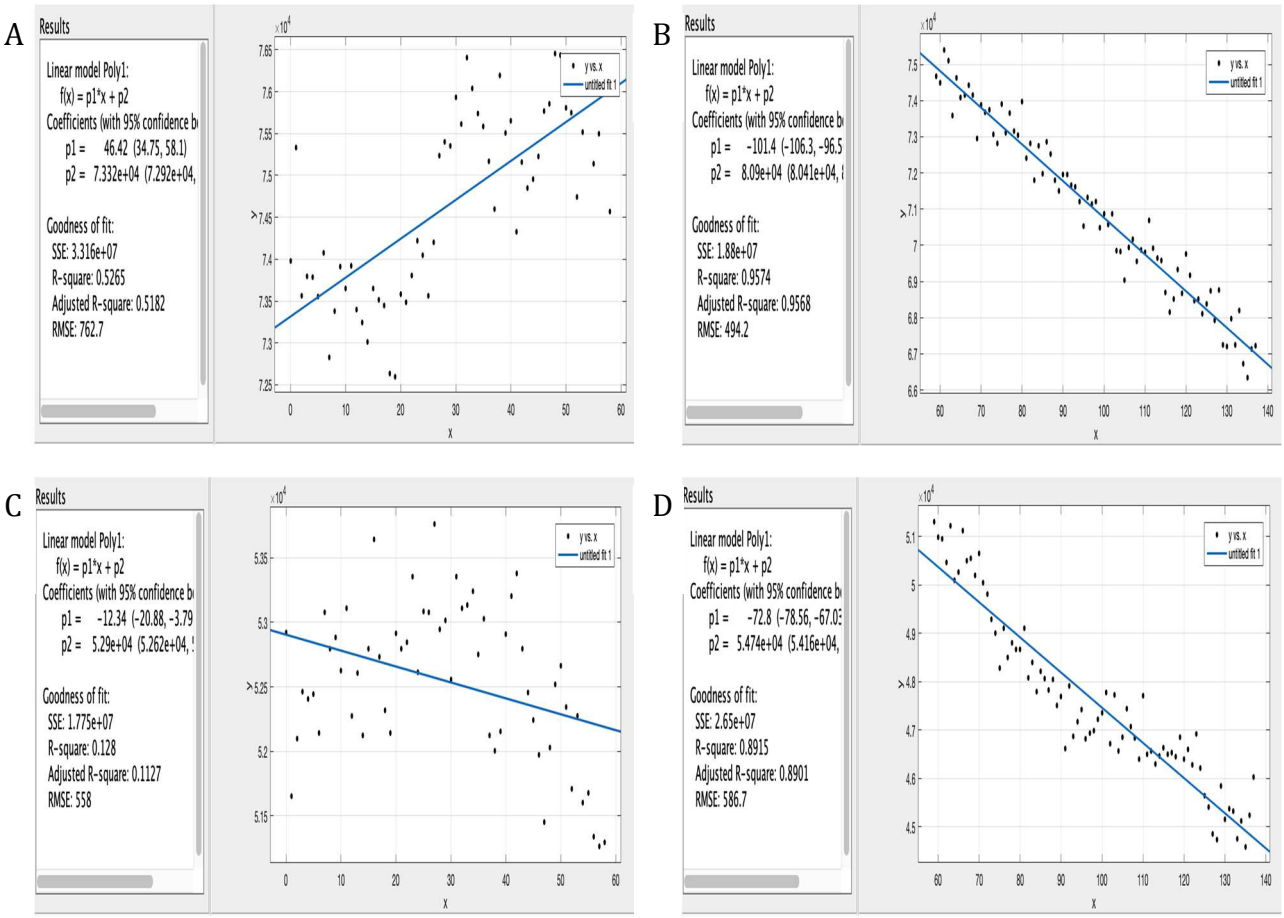

Figure S_{10} **10% water testing split trend-line graph at time point 60 seconds. A.** Baseline linear graph of integrated density vs. time (Pre-60s). **B.** Baseline linear graph of integrated density vs. time (Post-60s). **C.** Post-water addition linear graph of integrated density vs. time (Pre-60s). **D.** Post-water addition linear graph of integrated density vs. time (Post-60s).

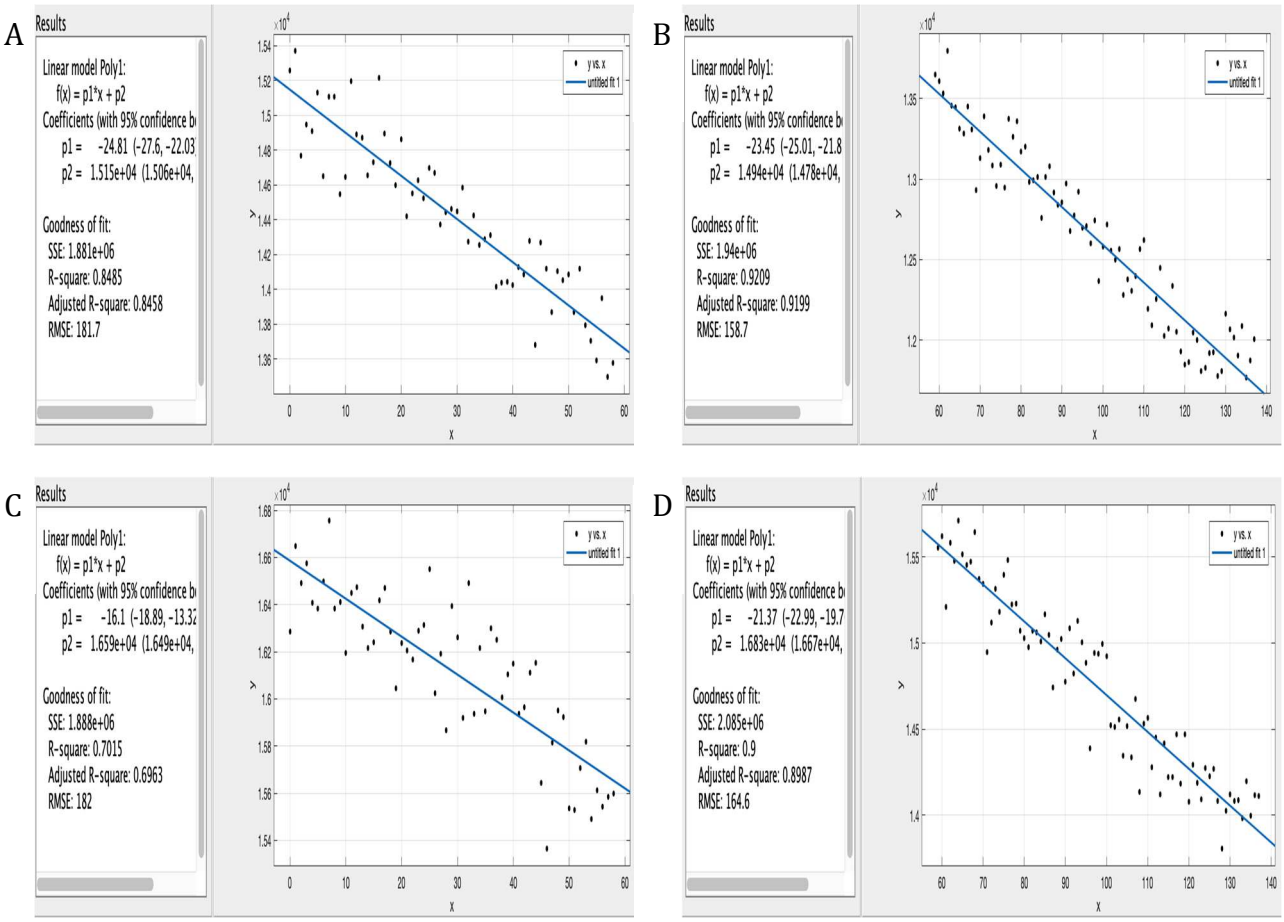

Figure S_{11} **25% water testing split trend-line graph at time point 60 seconds. A.** Baseline linear graph of integrated density vs. time (Pre-60s). **B.** Baseline linear graph of integrated density vs. time (Post-60s). **C.** Post-water addition linear graph of integrated density vs. time (Pre-60s). **D.** Post-water addition linear graph of integrated density vs. time (Post-60s).

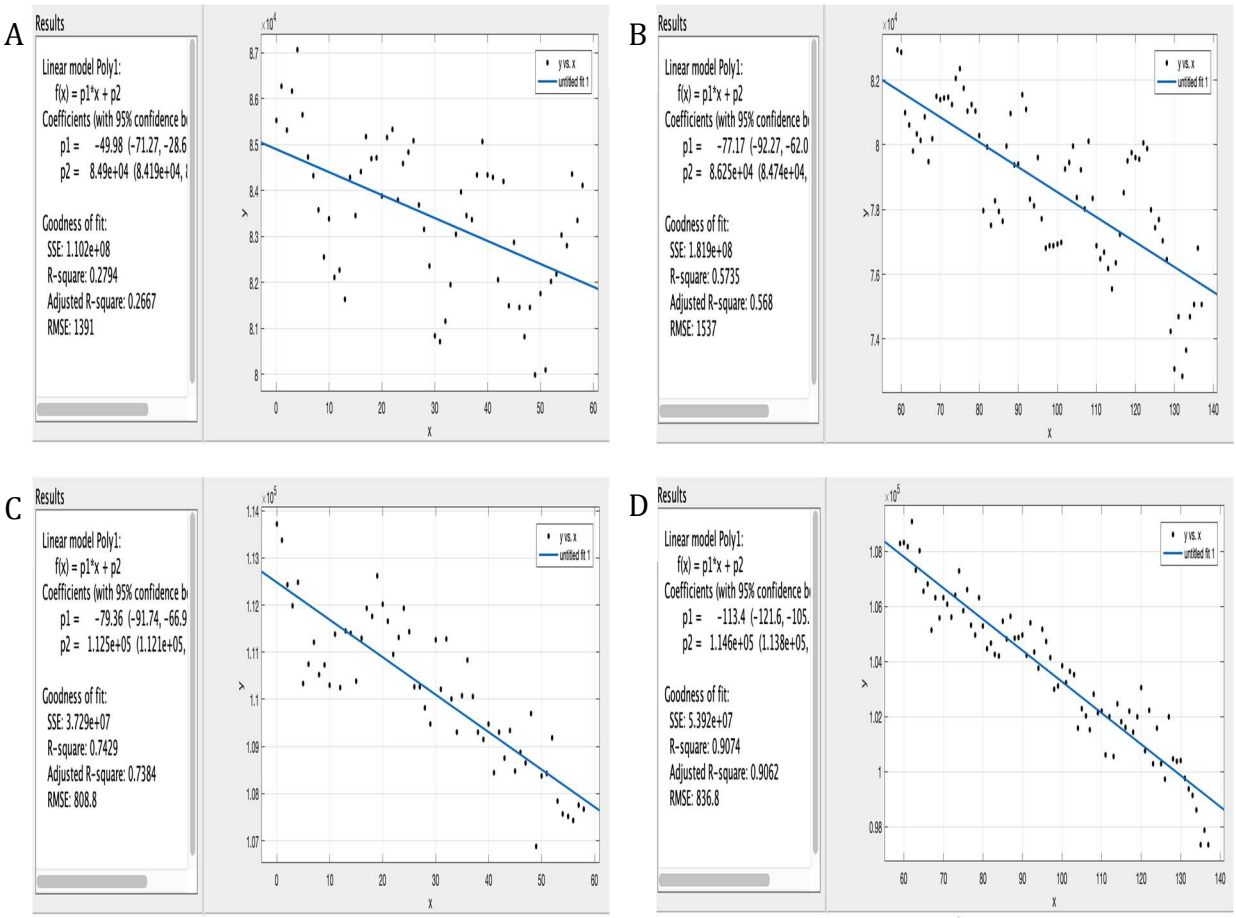

Figure S_{12} **50% water testing split trend-line graph at time point 60 seconds. A.** Baseline linear graph of integrated density vs. time (Pre-60s). **B.** Baseline linear graph of integrated density vs. time (Post-60s). **C.** Post-water addition linear graph of integrated density vs. time (Pre-60s). **D.** Post-water addition linear graph of integrated density vs. time (Post-60s).

A

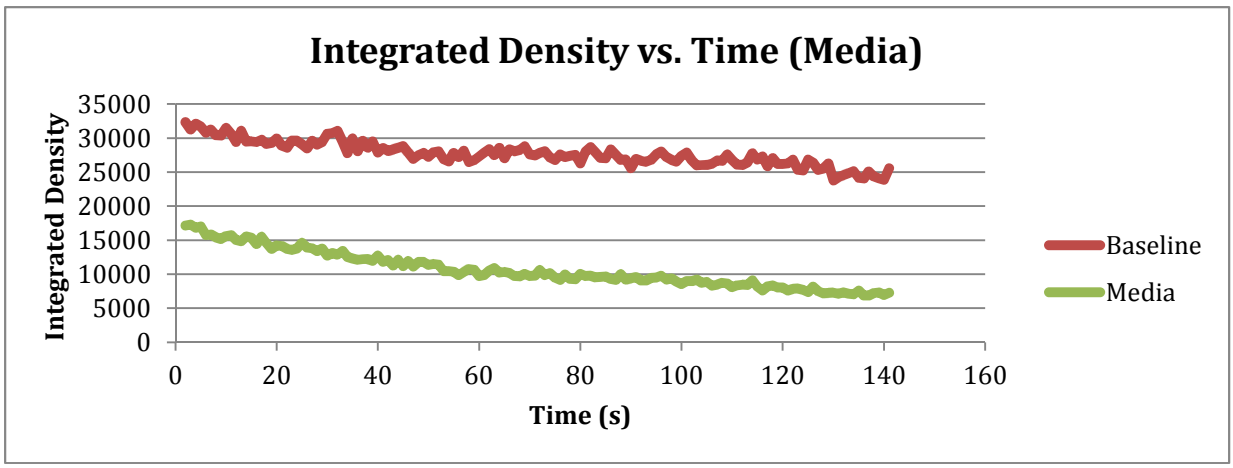

B

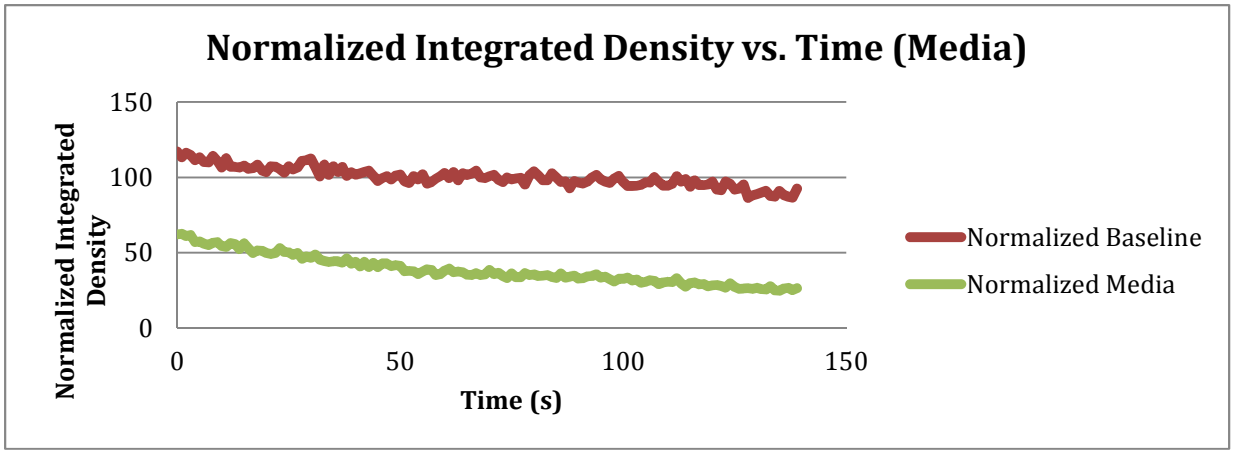

Figure S_{13} **HC-067047 media testing graphs. A.** Integrated density vs. time combined graph of baseline testing and with media addition. **B.** Normalized integrated density vs. time combined graph of baseline testing and with media addition. Normalized integrated density was taken by dividing the density value by cell area.

A

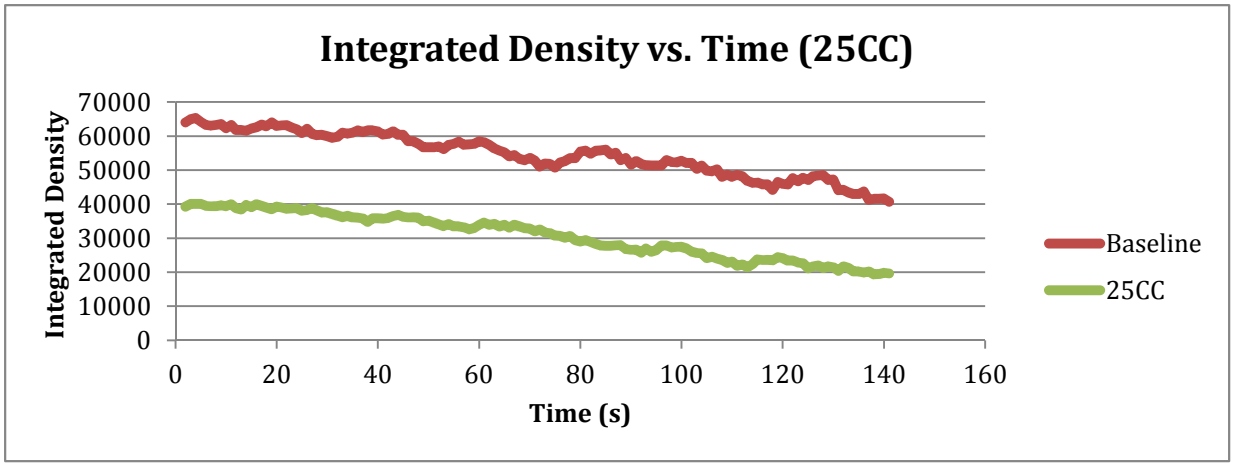

B

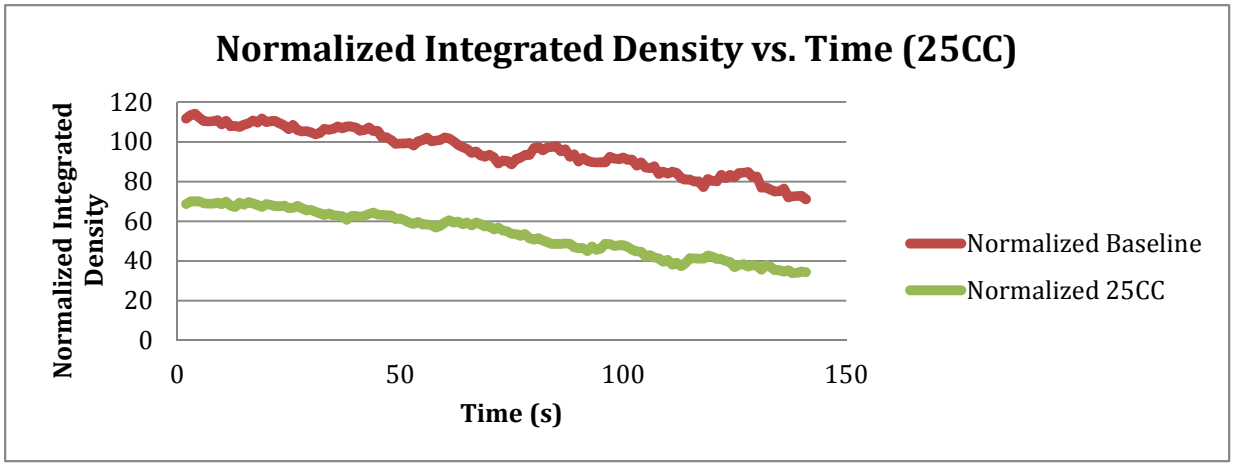

Figure S_{14} **HC-067047 25% water testing graphs. A.** Integrated density vs. time combined graph of baseline testing and with 25% water addition. **B.** Normalized integrated density vs. time combined graph of baseline testing and with 25% water addition. Normalized integrated density was taken by dividing the density value by cell area.

A

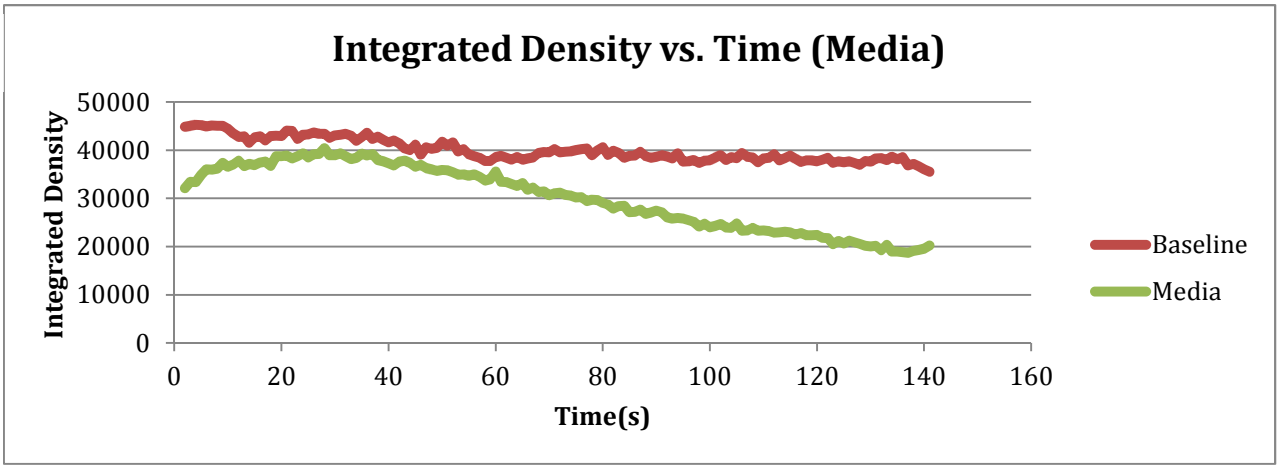

B

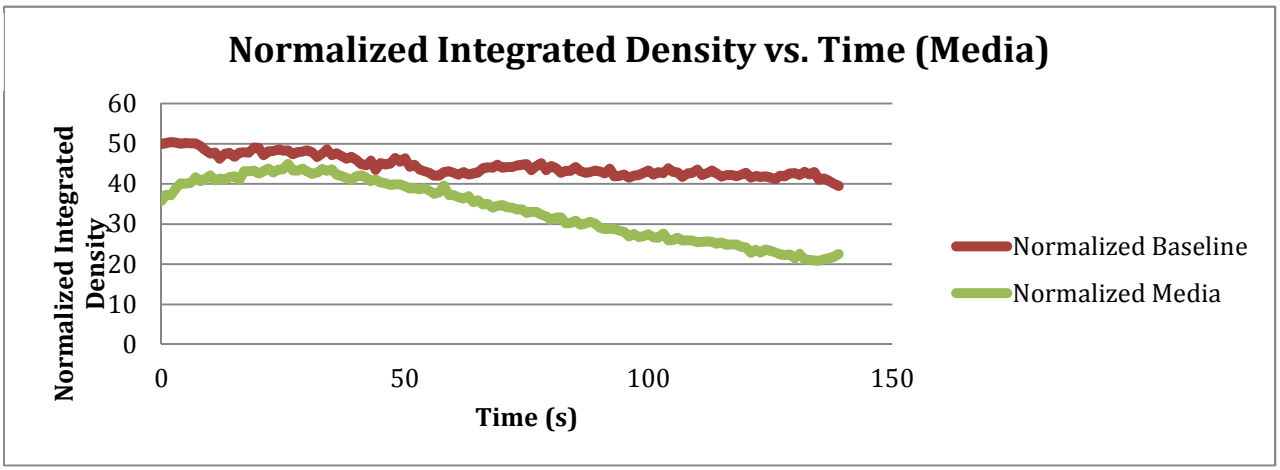

Figure S_{15} **GSK-2193874 media testing graphs. A.** Integrated density vs. time combined graph of baseline testing and with media addition. **B.** Normalized integrated density vs. time combined graph of baseline testing and with media addition. Normalized integrated density was taken by dividing the density value by cell area.

A

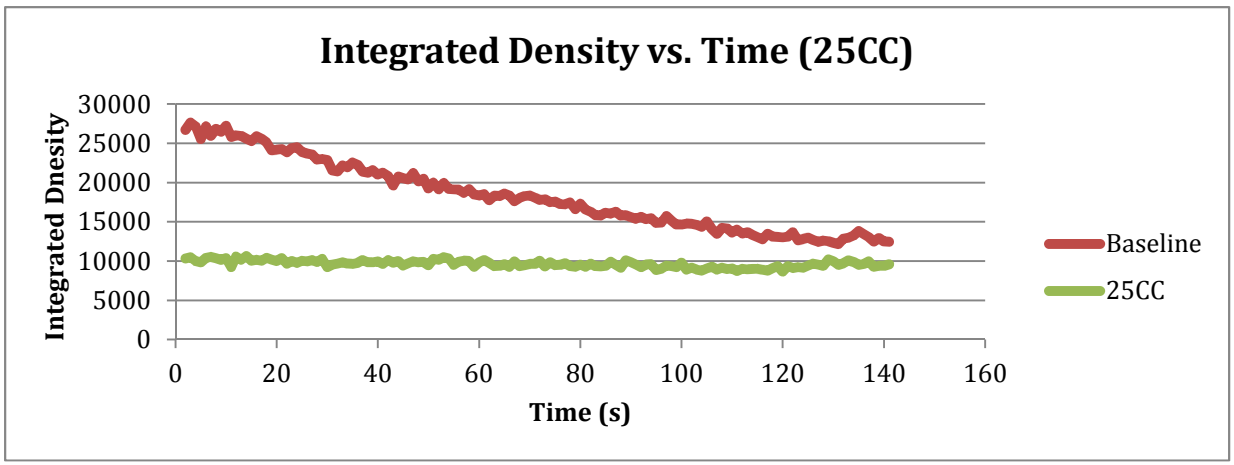

B

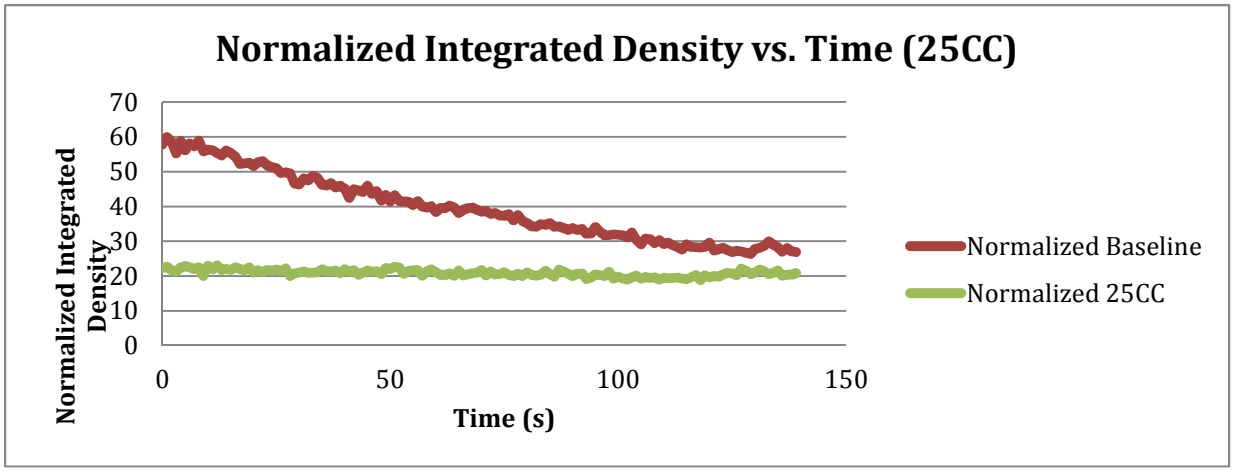

Figure S_{16} **GSK-2193874 25% water testing graphs. A.** Integrated density vs. time combined graph of baseline testing and with 25% water addition. **B.** Normalized integrated density vs. time combined graph of baseline testing and with 25% water addition. Normalized integrated density was taken by dividing the density value by cell area.

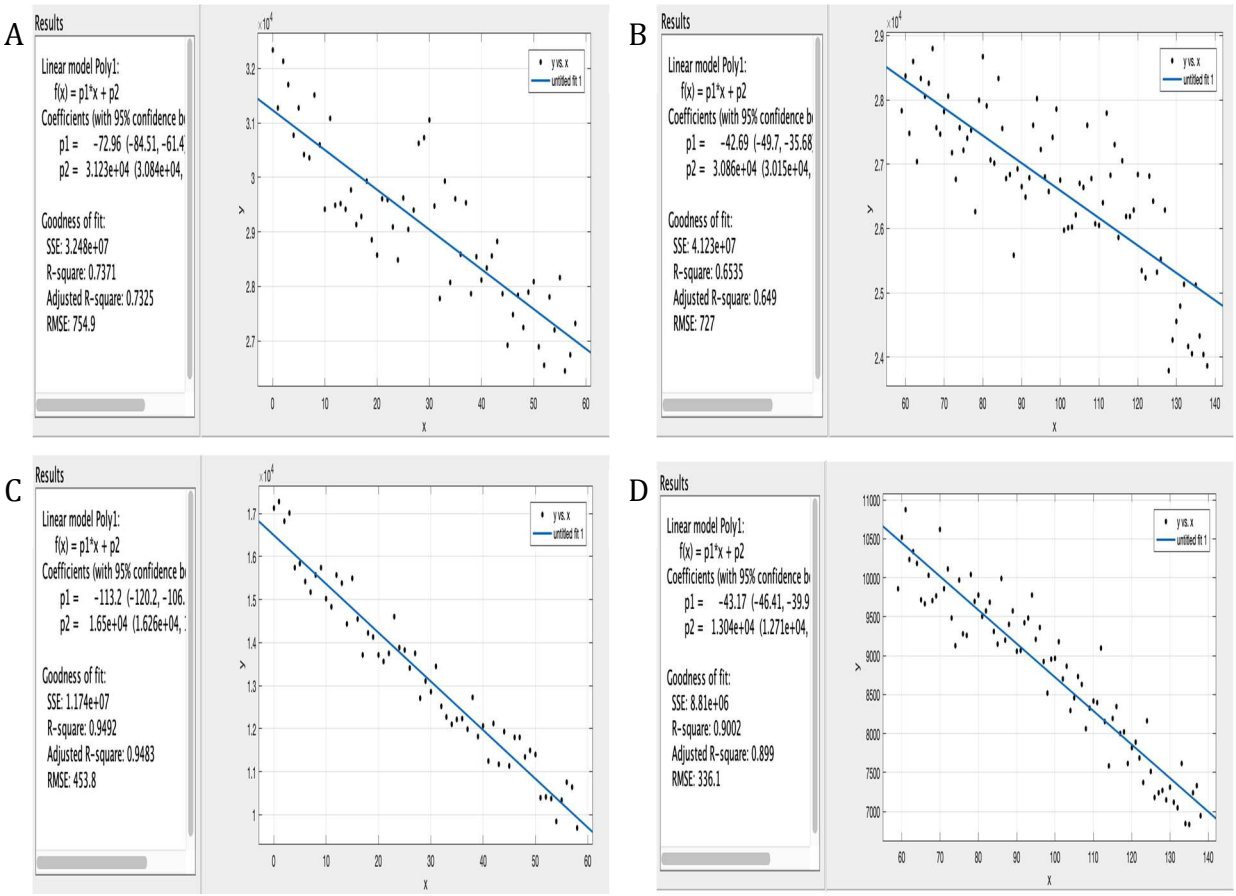

Figure S_{17} **HC-067047 media testing split trend-line graph at time point 60 seconds. A.** Baseline linear graph of integrated density vs. time (Pre-60s). **B.** Baseline linear graph of integrated density vs. time (Post-60s). **C.** Post-media addition linear graph of integrated density vs. time (Pre-60s). **D.** Post-media addition linear graph of integrated density vs. time (Post-60s).

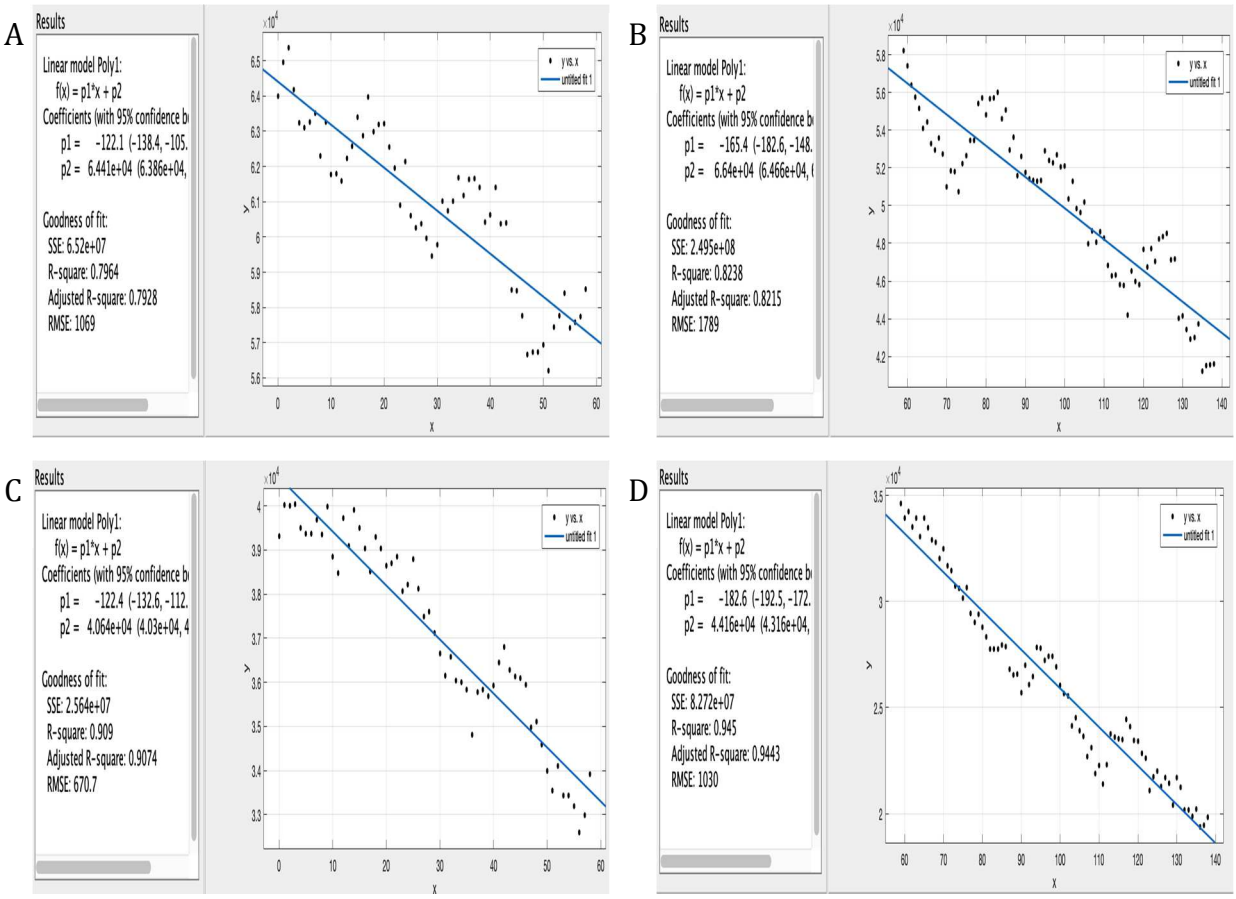

Figure S_{18} **HC-067047 25% water testing split trend-line graph at time point 60 seconds. A.** Baseline linear graph of integrated density vs. time (Pre-60s). **B.** Baseline linear graph of integrated density vs. time (Post-60s). **C.** Post-water addition linear graph of integrated density vs. time (Pre-60s). **D.** Post-water addition linear graph of integrated density vs. time (Post-60s).

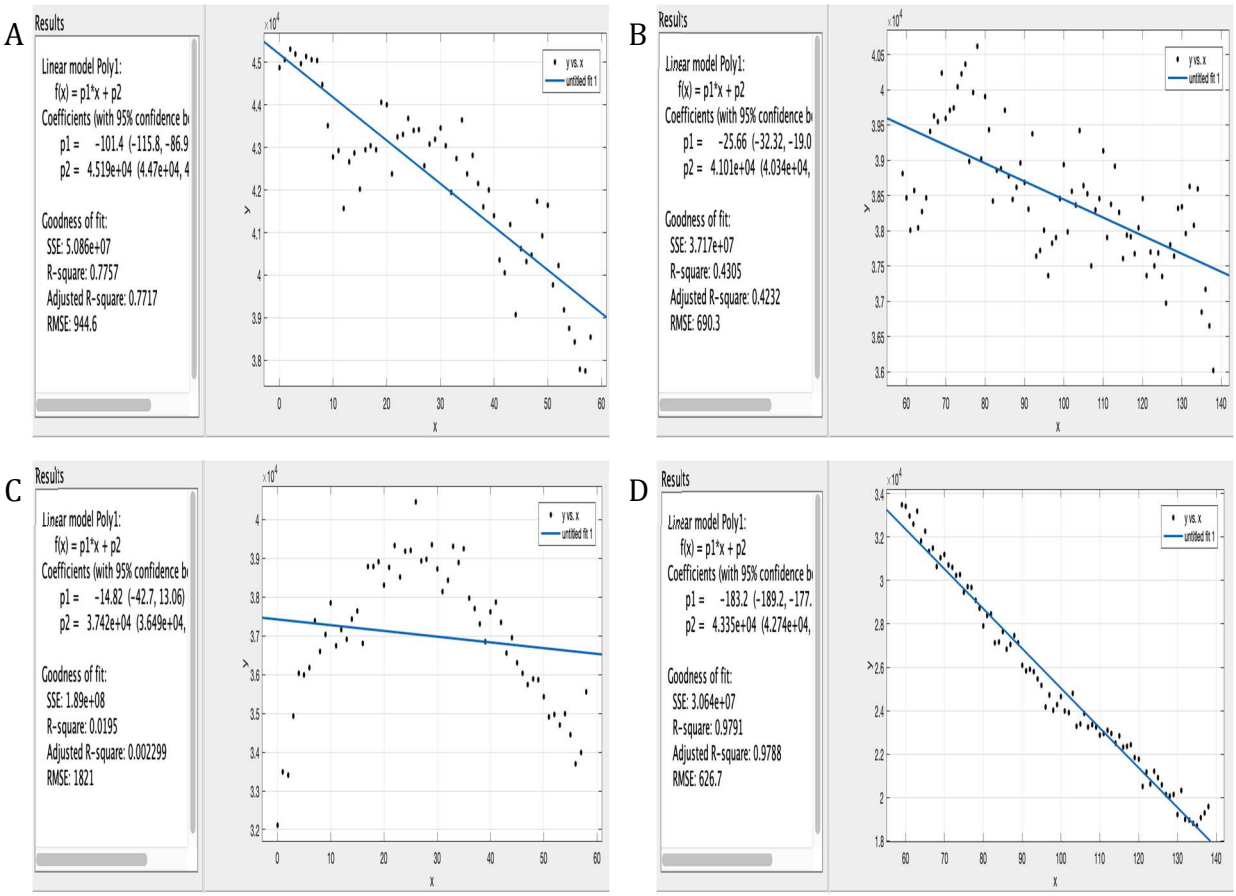

Figure S_{19} **GSK-2193874 media testing split trend-line graph at time point 60 seconds. A.** Baseline linear graph of integrated density vs. time (Pre-60s). **B.** Baseline linear graph of integrated density vs. time (Post-60s). **C.** Post-media addition linear graph of integrated density vs. time (Pre-60s). **D.** Post-media addition linear graph of integrated density vs. time (Post-60s).

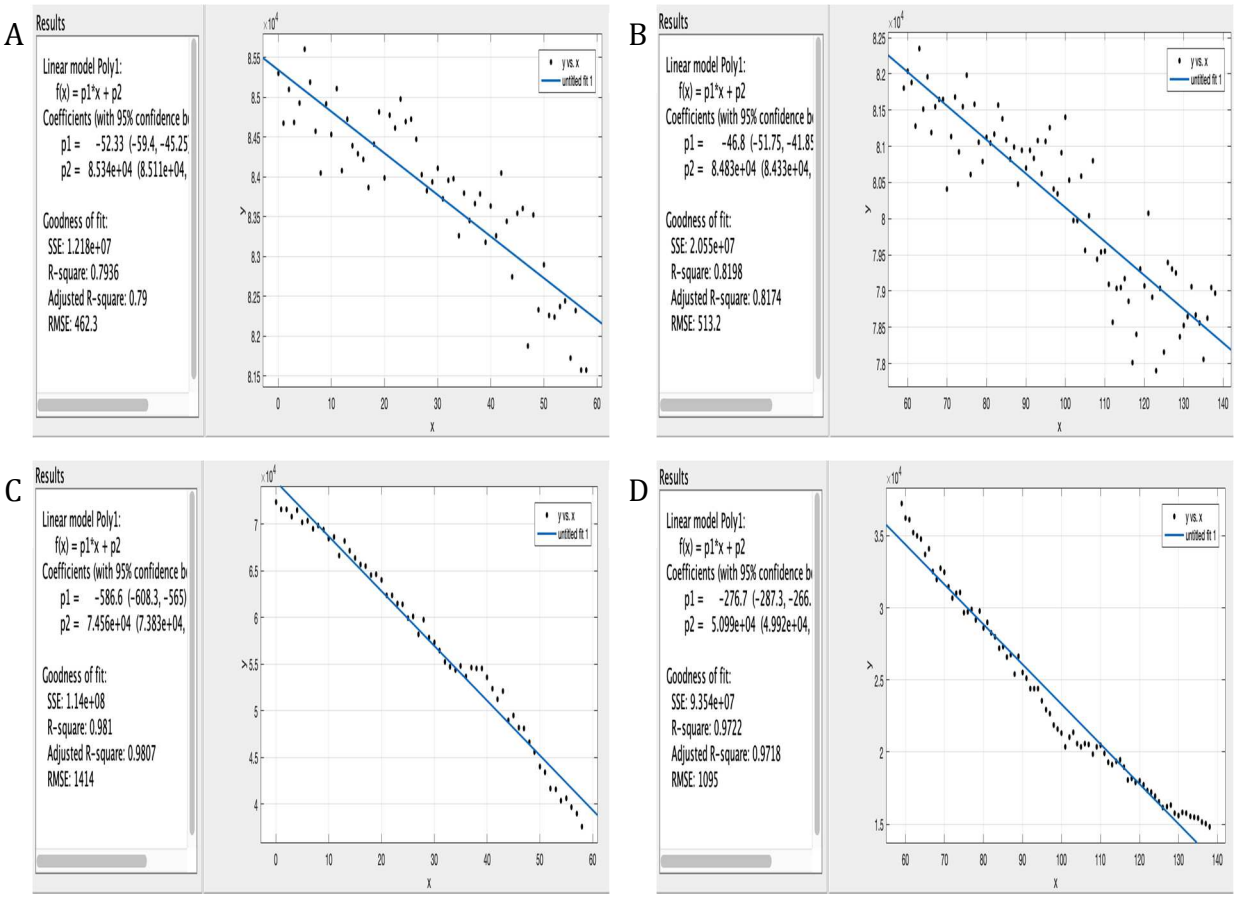

Figure S_{20} **GSK-2193874 25% water testing split trend-line graph at time point 60 seconds. A.** Baseline linear graph of integrated density vs. time (Pre-60s). **B.** Baseline linear graph of integrated density vs. time (Post-60s). **C.** Post-water addition linear graph of integrated density vs. time (Pre-60s). **D.** Post-water addition linear graph of integrated density vs. time (Post-60s).

A

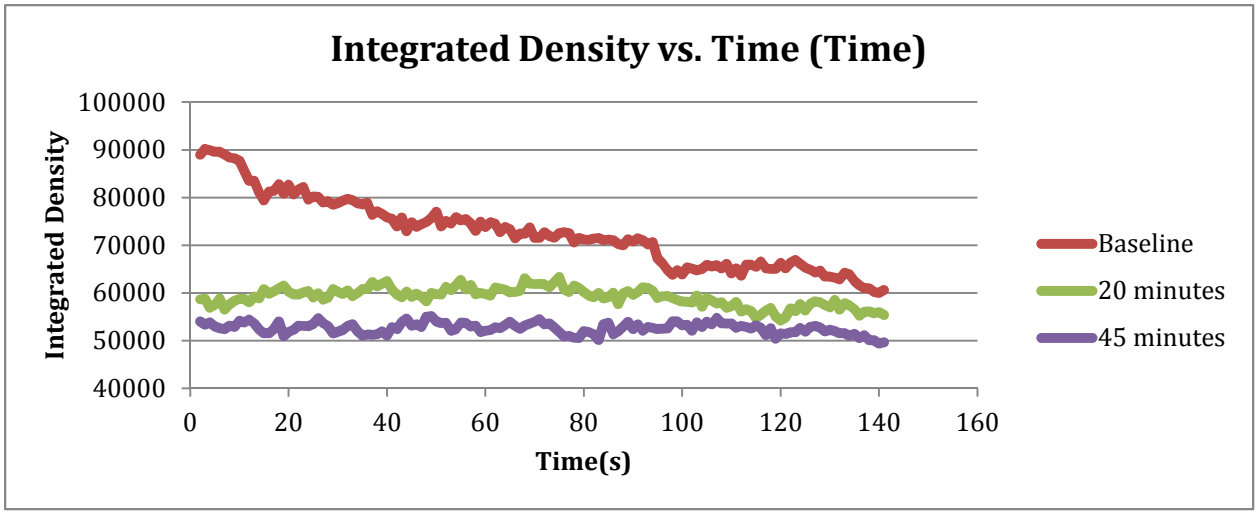

B

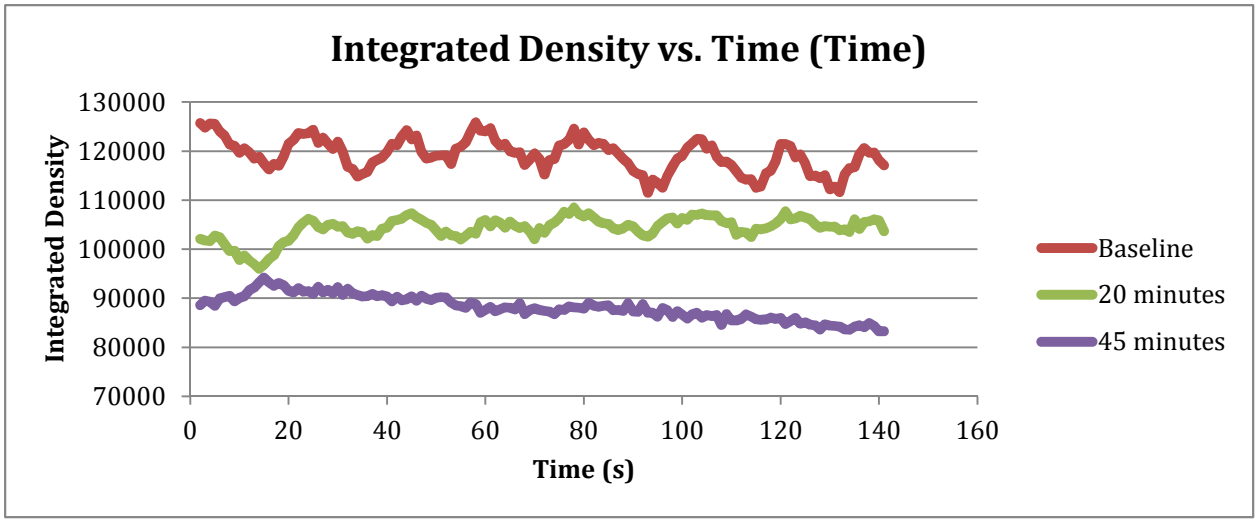

Figure S_{21} **Timed inhibitor effect testing graphs. A.** Integrated density vs. time combined graph of baseline testing, after 20 minutes, and after 45 minutes. **B.** Integrated density vs. time combined graph of baseline testing, after 20 minutes, and after 45 minutes.

References

[1] Zaorsky, N., Churilla, T., Egleston, B., Fisher, S., Ridge, J., Horwitz, E. and MD, J. (2016). Causes of death among cancer patients. *Annals of Oncology*, p.mdw604.

[2] Weaver, B. (2014). How Taxol/paclitaxel kills cancer cells. *Molecular Biology of the Cell*, 25(18), pp.2677-2681.

[3] Ludwig, P. E. and Varacallo, M. (n.d.). Neuroanatomy, Central Nervous System (CNS). *Neuroanatomy, Central Nervous System (CNS)*.

[4] Learning, L. (n.d.). Biology for Majors II. Retrieved from https://courses.lumenlearning.com/wm-biology2/chapter/the-central-and-peripheral-nervous-systems/

[5] Catala, M., & Kubis, N. (2013). Gross anatomy and development of the peripheral nervous system. *Handbook of Clinical Neurology Peripheral Nerve Disorders,*29-41. doi:10.1016/b978-0-444-52902-2.00003-5

[6] Yam, M., Loh, Y., Tan, C., Adam, S. K., Manan, N. A., & Basir, R. (2018). General Pathways of Pain Sensation and the Major Neurotransmitters Involved in Pain Regulation. *International Journal of Molecular Sciences, 19*(8), 2164. doi: 10.3390/ijms19082164

[7] Lodish H, Berk A, Zipursky. Molecular Cell Biology. 4th edition. New York: W. H. Freeman; 2000. Section 21.1, Overview of Neuron Structure and Function.

[8] OSC, M. F. (2017, September 15). Structure of a Neuron. Retrieved from https://owlcation.com/stem/Structure-of-a-Neuron

[9] Sapunar, D., Kostic, S., Banozic, A., & Puljak, L. (2012). Dorsal root ganglion – a potential new therapeutic target for neuropathic pain. *Journal of Pain Research,* 31. doi:10.2147/jpr.s26603

[10] Cooper GM. The Cell: A Molecular Approach. 2nd edition. Sunderland (MA): Sinauer Associates; 2000. The Development and Causes of Cancer.

[11] Hanahan, D., & Weinberg, R. A. (n.d.). Hallmarks of Cancer: The Next Generation.

[12] Baskar, R., Lee, K. A., Yeo, R., & Yeoh, K. (2012). Cancer and Radiation Therapy: Current Advances and Future Directions. *International Journal of Medical Sciences,9*(3), 193-199. doi:10.7150/ijms.3635

[13] Rosenbaum T, Simon SA. TRPV1 Receptors and Signal Transduction. In: Liedtke WB, Heller S, editors. TRP Ion Channel Function in Sensory Transduction and Cellular Signaling Cascades. Boca Raton (FL): CRC Press/Taylor & Francis; 2007. Chapter 5.

[14] Cao, S., Anishkin, A., Zinkevich, N. S., Nishijima, Y., Korishettar, A., Wang, Z., . . . Zhang, D. X. (2018). Transient receptor potential vanilloid 4 (TRPV4) activation by arachidonic acid requires protein kinase A–mediated phosphorylation. *Journal of Biological Chemistry, 293* (14), 5307-5322. doi:10.1074/jbc.m117.811075

15Li, L., Qu, W., Zhou, L., Lu, Z., Jie, P., Chen, L., & Chen, L. (2013). Activation of Transient Receptor Potential Vanilloid 4 Increases NMDA-Activated Current in Hippocampal Pyramidal Neurons. *Frontiers in Cellular Neuroscience,7*. doi:10.3389/fncel.2013.00017

[16]Cheung, M., Bao, W., Behm, D. J., Brooks, C. A., Bury, M. J., Dowdell, S. E., Eidam, H.S., Fox, R.M., Goodman K.B., Holt, D.A., Lee, D., Roethke, T.J., Willette, R.N., Xu X., Ye, G.,Thorneloe, K. S. (2017). Discovery of GSK2193874: An Orally Active, Potent, and Selective Blocker of Transient Receptor Potential Vanilloid 4. *ACS Medicinal Chemistry Letters,8*(5), 549-554. doi:10.1021/acsmedchemlett.7b00094

[17]HC-067047 SML0143. (n.d.). Retrieved from https://www.sigmaaldrich.com/catalog/product/sigma/sml0143?lang=en®ion=US&gclid=Cj0KCQjwov3nBRDFARIsANgsdoGVVjJc-nXHjQMXT1q69eChVIej7NOu37JKNqJgj81Qw-hAuwBlVEIaAv3_EALw_wcB

[18]GSK2193874 SML0942. (n.d.). Retrieved from https://www.sigmaaldrich.com/catalog/product/sigma/sml0942?lang=en®ion=US&gclid=Cj0KCQjwxYLoBRCxARIsAEf16-u0OpvTVT2X4OYNt75BWPzIDttA_dVlx3DVX3QMJnbWV9F5K2pzqRYaAnD5EALw_wcB

[19]Kitagawa, C., Nakatomi, A., Hwang, D., Osaka, I., Fujimori, H., Kawasaki, H., Arakawa R., Murakami, Y., Ohki, S. (2011). Roles of the C-terminal residues of calmodulin in structure and function. *Biophysics,7*, 35-49. doi:10.2142/biophysics.7.35

[20] Misra, U. K., Kalita, J., & Nair, P. P. (2008). Diagnostic approach to peripheral neuropathy. *Annals of Indian Academy of Neurology*, *11*(2), 89–97. doi:10.4103/0972-2327.41875

[21] Hallett, M., Tandon, D., & Berardelli, A. (1985). Treatment of peripheral neuropathies. *Journal of neurology, neurosurgery, and psychiatry*, *48*(12), 1193–1207. doi:10.1136/jnnp.48.12.1193

[22] Kadavath, H., Hofele, R. V., Biernat, J., Kumar, S., Tepper, K., Urlaub, H., Mandelkow E., Zweckstetter, M. (2015). Tau stabilizes microtubules by binding at the interface between tubulin heterodimers. *Proceedings of the National Academy of Sciences, 112*(24), 7501-7506. doi:10.1073/pnas.1504081112

[23] Gozes, I. (2011). Microtubules (tau) as an Emerging Therapeutic Target: NAP (Davunetide). *Current Pharmaceutical Design, 17*(31), 3413-3417. doi:10.2174/138161211798072553

[24]Yusaf, S. P., Goodman, J., Pinnock, R. D., Dixon, A. K., & Lee, K. (2001). Expression of voltage-gated calcium channel subunits in rat dorsal root ganglion neurons. *Neuroscience Letters,311*(2), 137-141. doi:10.1016/s0304-3940(01)02038-9

[25]Ranade, S., Syeda, R., & Patapoutian, A. (2015). Mechanically Activated Ion Channels. *Neuron,88*(2), 433. doi:10.1016/j.neuron.2015.10.016

[26] Li, Y., Tatsui, C. E., Rhines, L. D., North, R. Y., Harrison, D. S., Cassidy, R. M., Johansson, C. A., Kosturak, A. K., Edwards, D. D., Zhang, H., Dougherty, P. M. (2017). Dorsal root ganglion neurons become hyperexcitable and increase expression of voltage-gated T-type calcium channels (Cav3.2) in paclitaxel-induced peripheral neuropathy. *Pain,158*(3), 417-429. doi:10.1097/j.pain.0000000000000774

[27]Zhang, M., Wang, Y., Geng, J., Zhou, S., & Xiao, B. (2019). Mechanically Activated Piezo Channels Mediate Touch and Suppress Acute Mechanical Pain Response in Mice. *Cell Reports,26*(6). doi:10.1016/j.celrep.2019.01.056

[28]Zhang, Y., Laumet, G., Chen, S., Hittelman, W. N., & Pan, H. (2015). Pannexin-1 Up-regulation in the Dorsal Root Ganglion Contributes to Neuropathic Pain 28Development. *Journal of Biological Chemistry,290*(23), 14647-14655. doi:10.1074/jbc.m115.650218

[29]Hdud, I. M., Mobasheri, A., & Loughna, P. T. (2014). Effect of osmotic stress on the expression of TRPV4 and BKCa channels and possible interaction with ERK1/2 and p38 in cultured equine chondrocytes. *American Journal of Physiology-Cell Physiology,306*(11). doi:10.1152/ajpcell.00287.2013

[30] Sleigh, J. N., Weir, G. A., & Schiavo, G. (2016). A simple, step-by-step dissection protocol for the rapid isolation of mouse dorsal root ganglia. *BMC Research Notes,9*(1). doi:10.1186/s13104-016-1915-8

[31] Maqboul, A., & Elsadek, B. (2018). Expression profiles of TRPV1, TRPV4, TLR4 and ERK1/2 in the dorsal root ganglionic neurons of a cancer-induced neuropathy rat model. *PeerJ, 6*. doi:10.7717/peerj.4622